Synthesis, antidiabetic activity and molecular docking study of rhodanine-substitued spirooxindole pyrrolidine derivatives as novel α-amylase inhibitors

Amani Toumi, Sarra Boudriga, Khaled Hamden, Mansour Sobeh, Mohammed Cheurfa, Moheddine Askri, Michael Knorr, Carsten Strohmann, Lukas Brieger

Synthesis, antidiabetic activity and molecular docking study of rhodanine-substitued spirooxindole pyrrolidine derivatives as novel α-amylase inhibitors.

Amani Toumi[a], Sarra Boudriga[a], Khaled Hamden[b], Mansour Sobeh[c], Mohammed Cheurfa[d], Moheddine Askri[a*], Michael Knorr[e*], Carsten Strohmann[f], Lukas Brieger[f]

[a]*Laboratory of Heterocyclic Chemistry Natural product and Reactivity/CHPNR, Department of Chemistry, Faculty of Science of Monastir, 5000 Monastir, Tunisia; Email:moheddine.askri@fsm.rnu.tn.*

[b]*Laboratory of Bioresources: Integrative Biology and Valorization, Higher Institute of Biotechnology of Monastir, University of Monastir, Tunisia.*

[c] *Departement of Biology, Faculty of Nature, Life and Earth Sciences, University of Djillali Bounaama, Khemis Miliana Road Teniet Elhad, Khemis Miliana 44225, Algeria.*

[d]*AgroBioSciences Research Division, Mohammed VI Polytechnic University, Lot 660–Hay Moulay Rachid, Ben-Guerir 43150, Morocco.*

[e]*Institut UTINAM - UMR CNRS 6213, Université Bourgogne Franche-Comté, 16 Route de Gray, 25030 Besançon, France ; Email:michael.knorr@univ-fcomte.fr.*

[f]*Technische Universität Dortmund, Anorganische Chemie, Otto-Hahn-Strasse 6, 44227 Dortmund, Germany.*

ABSTRACT: In a sustained search for novel α-amylase inhibitors for the treatment of type 2 diabetes mellitus (T2DM), we report herein the synthesis of a series of nineteen novel rhodanine-fused spiro[pyrrolidine-2,3'-oxindoles]. They were obtained by *one-pot* three component [3+2] cycloaddition of stabilized azomethine ylides, generated *in situ* by condensation of glycine methyl ester and the cyclic ketones 1*H*-indole-2,3-dione (isatin), with *(Z)*-5-arylidine-2-thioxothiazolidin-4-ones. The highlight of this protocol is the efficient high-yield construction of structurally diverse rhodanine-fused spiro[pyrrolidine-2,3'-oxindoles] scaffolds, including four contiguous stereocenters, along with excellent regio- and diastereoselectivities. The stereochemistry of all compounds was confirmed by NMR and corroborated by an X-ray diffraction study performed on one derivative. All cycloadducts were evaluated *in vitro* for their α-amylase inhibitory activity and showed good α-amylase inhibition with IC_{50} values ranging between 1.49± 0.10 and 3.06± 0.17µM, with respect to the control drug acarbose (IC_{50}= 1.56µM). Structural activity relationships (SARs) were also established for all synthesized compounds and the binding interactions of the most active spiropyrrolidine derivatives were modelled by means of molecular *in silico* docking studies. The most potent compounds **5g**, **5k**, **5s** and **5l** were further screened *in vivo* for their hypoglycemic activity in alloxan-induced diabetic rats, showing a reduction of the blood glucose level. Therefore, these spiropyrrolidine derivatives may be considered as promising candidates for the development of new classes of antidiabetic drugs.

Keywords**:** *Spirooxindole pyrrolidine; Rhodanine; Antidiabetic; α-Amylase; 1,3-Dipolar cycloaddition; Structure-activity relationship (SAR); Molecular docking*

1. Introduction

Type 2 diabetes mellitus (T2DM) is a serious chronic metabolic disorder manifested by elevated blood glucose levels caused by inadequate insulin secretion or insulin resistance [1]. With the rapid increase of people suffering from T2DM, it has become a major health problem worldwide. It affects approximately 425 million of the global population in 2017 and has been estimated to increase by 629 million in 2045. Twelve percent of global healthcare expenditure, 727 billion dollars, is spent on diabetes [2]. Chronic hyperglycemic sufferers have to live with a high risk of micro- and macrovascular complications. Cardiovascular diseases, retinopathy, nephropathy, and neuropathy, are the main important characters of T2DMand represent a major risk for the development of diabetes [3-5]. These chronic complications may lead to coronary heart disease, stroke and other blood vessel diseases, nerve damage, kidney failure, and ophthalmic infections with time [6-8].

One of the relevant therapeutic approaches introduced for prevention of T2DM is the inhibition of the activity of the *α*-amylase enzyme to reduce the absorption of glucose in intestines[9].*α*-Amylase (*α-1,4*-d-glucan glucanohydrolases) is a amylolytic enzyme, secreted from salivary gland and pancreas participating in the hydrolysis of the insoluble starch complex to oligosaccharides in the intestinal mucosa. For this purpose, inhibition of this enzyme can effectively delay the liberation of glucose into the bloodstream and thus the management of degenerative health problems such as T2DM [10].

To date, multiple drugs have been introduced for the treatment of T2DM including metformin, sulfonylureas and thiazolidinediones (TZDs) [11-13]. These medicines are used alone as monotherapy or in combination if the goal of achieving glycemic control is not achieved [14]. TZDs (rosiglitazone, pioglitazone) are insulin-sensitizing drugs used in T2DM that bind the peroxisome proliferator-activated receptor-gamma (PPAR-γ), which is an important regulator of blood glucose level and dyslipidemia with minimal risk of hypoglycemia [15-17].

As one of the thiazolidines subtypes, rhodanines (2-thioxothiazolidin-4-ones) have been attracting much attention in medicinal and pharmaceutical chemistry [18,19]. These moleculeshave been reported as, *e.g.*,HIV-1 Integrase Inhibitors [20],topoisomerase II inhibition potency [21], anticancer activity against MCF-7 breast cancer[22]and potential

cholinesterase inhibitors [23,24]. Among all of these, the treatment of T2DM and its related complications are the most investigated therapeutic activities of rhodanines after approval of Epalrestat clinically used as inhibitor drug of aldose reductase (ALR) enzyme (Fig.1) [25]. So far, several rhodanine derivatives have been also identified as potential inhibitors of essential therapeutic targets such as α-amylase[26], PTP1B [27] and α-glucosidase [28] for the clinical management of T2DM (Fig.1).

Consequently, chemical modification and pharmacological evaluation of these molecules is still of high actuality.

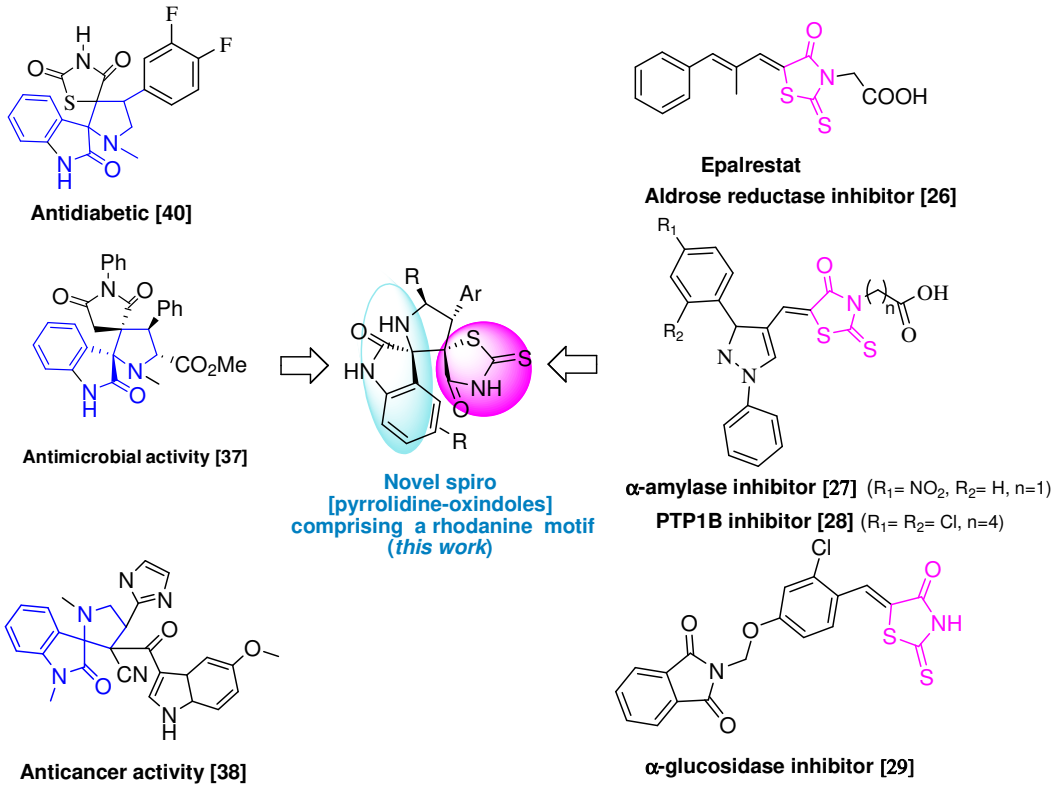

Fig.1. Examples of bioactive molecules containing rhodanine and spiro[pyrrolidine–oxindole] units.

1,3-dipolar cycloaddition of azomethine ylides across electron-deficient dipolarophiles is established as a powerful strategy for the synthesis of structurally prominent spiroxindole pyrrolidine derivatives that make part of many pharmaceutical and natural products [29-31]. In particular, spiro[pyrrolidin-2,3'-oxindoles] have emerged as attractive synthetic targets, since their widespread panoply of significant bioactivities covers antimicrobial [32], anticancer [33], cholinesterase inhibition activities [34] and antidiabetic ones [35] (Fig.1).Their prevalence in privileged structures has attracted a salient synthetic interest. Up to now, only a few methods have been described in literature for the synthesis of rhodanine-substituted-spiro[pyrrolidine-oxindole] derivatives by 1,3-dipolar cycloaddition reactions [35-37]. Despite these recent

advances, a 1,3-dipolar cycloaddition of stabilized azomethine ylides generated *in situ* by thermal [1,5]-prototropy with rhodanine has yet not been reported for the synthesis of the related rhodanine-linked- spirooxindole compounds (Scheme 1).

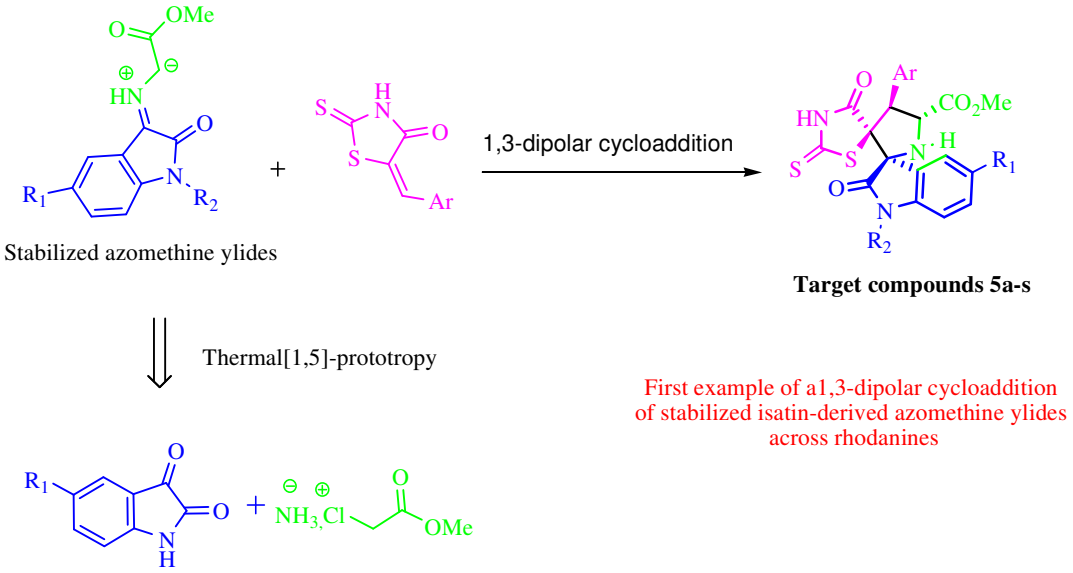

Scheme 1. Strategy for the construction of novel rhodanine-fused spiro[pyrrolidine-2,3'-oxindoles].

In our continuous effort on the design of new bioactive heterocyclic scaffolds for biological screenings [30,32,38], we highlight herein the synthesis of an extended series of nineteen spiro[pyrrolidine-2,3'-oxindole] derivatives *via* one-pot three-component 1,3-dipolar cycloaddition reactions of stabilized azomethine ylides across rhodanine. The current protocol provides a facile and efficient approach for the incorporation of rhodanine and spiro[pyrrolidine-2,3'-oxindole] scaffolds, allowing the formation of several new covalent bonds in only one single step, effectively well adapted for combinatorial synthesis.

The synthetic work presented in our contribution is completed by the *in vitro* investigation of the antidiabetic activity of this novel family of spiro[pyrrolidine-oxindole] derivatives against the α-amylase enzyme. The structure-activity relationships (SAR) of designed compounds is also discussed. A molecular docking study was performed in order to understand the binding interactions of the most active analogs with the active site of the α-amylase enzyme. Furthermore, an *in vivo* antidiabetic study was conducted. For this purpose, compounds **5g**, **5k**, **5s** and **5l** were orally administered to alloxan-induced diabetic rats.

2. Results and discussion

2.1.Synthetic Chemistry

We started our investigation by carrying out the reaction of *(Z)*-5-arylidene-2-thioxothiazolidin-4-one **1a** with stabilized azomethine ylides, generated *in situ* by thermal [1,5]-prototropy of isatin **2a** with glycine methyl ester chloride **3**, as a model substrate (Scheme 2). The 5-arylidenerhodanines **1a-f** have been prepared *via* base-catalyzed Knoevenagel condensation reaction between rhodanines and diverse aromatic aldehydes [39]. This three-component reaction was conducted under various conditions in order to optimize the reaction parameters (Table 1). Reaction temperature, time, solvents with varying polarity and different bases were screened, and the results are summarized in Table 1. Initially, the reaction was conducted in MeOH in the presence of different bases such as NEt_3, K_2CO_3, DABCO, and NH_4OAc (Table 1, *entries 1, 3* and *4*). Among all probed bases, NEt_3 was found to be the most suitable one for this reaction. (Table 1, *entry 1*). When the reaction temperature was lowered from reflux to room temperature, no reaction occurred even after 24h (Table 1, *entry 2*). Subsequently, a survey of various solvents, using NEt_3 as base, was performed and revealed acetonitrile to be the best reaction medium, providing higher yields and shorter reaction time (Table 1, *entry 8*). No significant increase in yield could be achieved when increasing the reaction time from 2 h to 8 h (65% vs. 64% yields, respectively, *entries 1* and *5*). We also noticed that the use of only a 0.05 mmol of the organic base (NEt_3) was not beneficial for the reaction yield (Table 1, *entry 11*). As shown in Table 1, best results were obtained by refluxing the reaction mixture in acetonitrile for 2 hours, providing the spiropyrrolidine **5a** in very satisfying yield (80%) (Table 1, *entry 8*).

Scheme 2. 1,3-Dipolar cycloaddition leading to spirooxindole pyrrolidine **5a.**

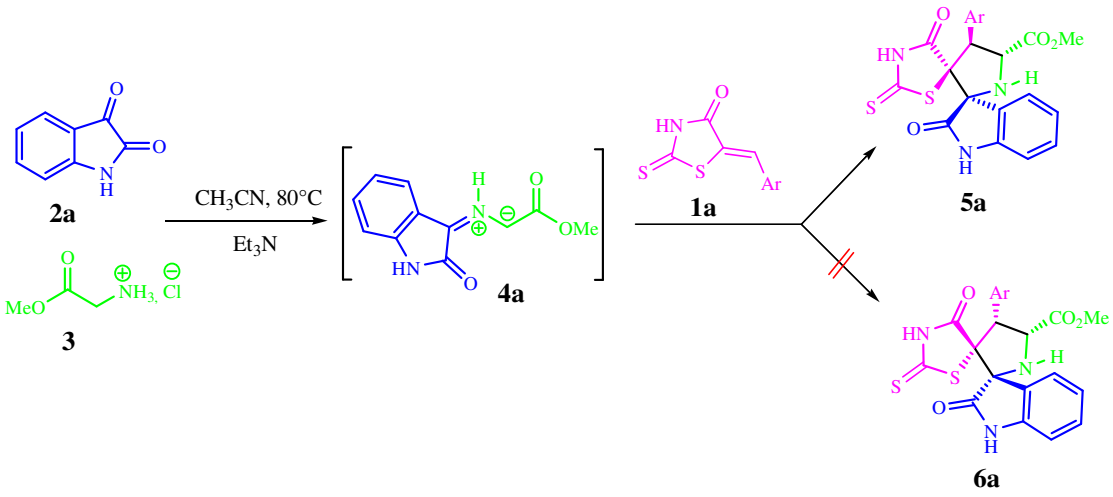

Table 1. Optimization of the reaction conditions [a].

Entry	*Solvent*	*Time (h)*	*t(°c)*	*Base*	**Yield[b](%)**
1	MeOH	2	reflux	NEt_3	65
2	MeOH	24	25	NEt_3	NR[c]
3	MeOH	2	reflux	K_2CO_3	60
4	MeOH	2	reflux	NH_4OAc	57
5	MeOH	8	reflux	NEt_3	64
6	Toluene	2	65	NEt_3	25
7	EtOH	2	reflux	NEt_3	62
8	**CH_3CN**	**2**	**80**	**NEt_3**	**80**
9	H_2O	24	70	NEt_3	NR[c]
10	THF	2	78	NEt_3	55
11[d]	CH_3CN	2	reflux	NEt_3	33

[a] Unless otherwise noted, all reactions were carried out with **1a**(0.1 mmol), **2a**(0.1 mmol), **3** (0.1 mmol), and base (0.1 mmol) in solvent (1.0 mL) at specified temperature. [b] Isolated yield. [c] No reaction. [d] Reaction was carried out with 0.05 mmol of NEt_3.

Once the optimal reaction conditions established (Table 1, entry 8), we examined the scope of the cycloaddition reaction with regard to the diverse dipolarophiles **1** and cyclic ketones **2** (Table 2). Both electron-donating and electron-withdrawing groups at the aryl units of the Knoevenagel adduct **1**(H, CH_3, OCH_3, F, Cl and Br) were well tolerated. Results revealed that the desired pyrrolidine-fused spirooxindole cycloadducts can be obtained in relatively high yields and selectivities (*dr* = 100%) from different sets of substrates (Table 2). Notably, substituted isatins with electron-withdrawing functional groups including Cl, Br and NO_2 (5-substitution) exhibited good performance and delivered the corresponding products in good yields along with excellent diastereoselectivities (Table 2). Furthermore, when isatin **2a** was replaced with *N*-benzyl-substituted isatin **2e**, a significant positive influence on the reaction was observed affording considerably improved yields (Table 2).

Table 2. Substrate Scope.[a]

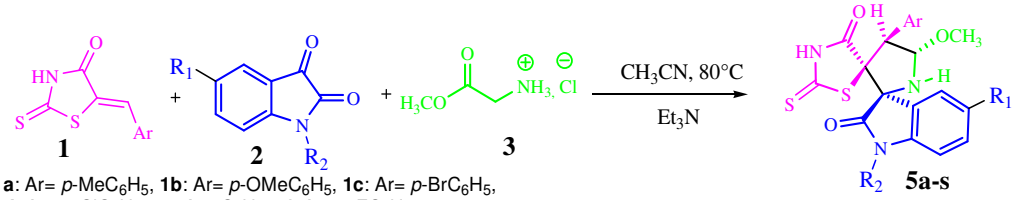

1a: Ar= *p*-MeC_6H_5, **1b**: Ar= *p*-$OMeC_6H_5$, **1c**: Ar= *p*-BrC_6H_5,
1d: Ar= *p*-ClC_6H_5, **1e**: Ar= C_6H_5, **1f**: Ar= *p*-FC_6H_5
2a: R_1= H,R_2= H, **2b**: R_1= Cl,R_2= H, **2c**: R_1= Br,R_2= H,
2d: R_1= NO_2, R_2= H, **2e**: R_1= H,R_2= Bn

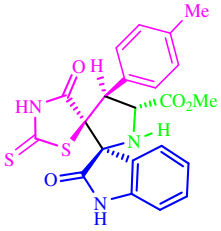

5a , 80%

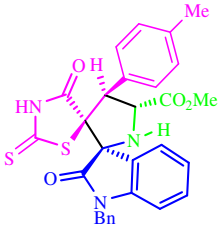

5b , 95%

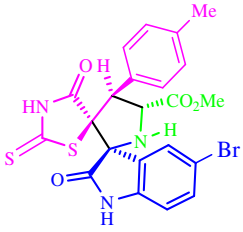

5c , 86%

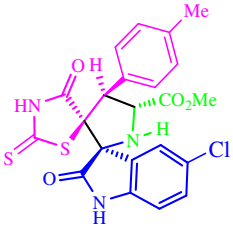

5d , 83%

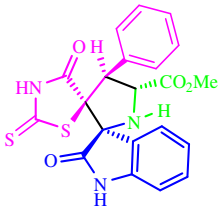

5e , 85 %

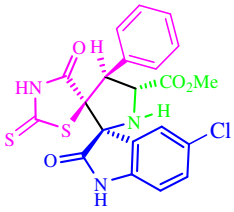

5f , 88%

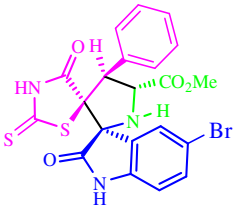

5g , 91 %

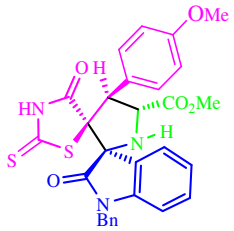

5h , 75%

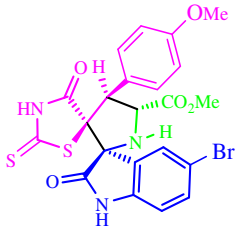

5i, 66%

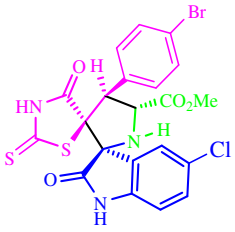

5j, 81 %

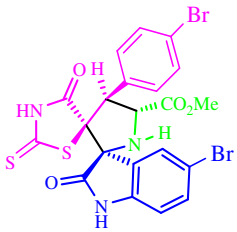

5k , 85%

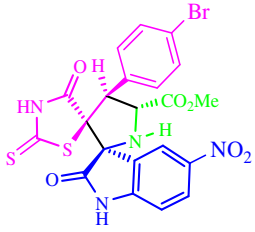

5l, 83%

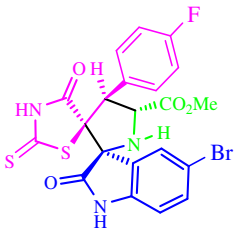

5m , 84%

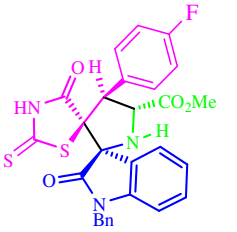

5n , 94%

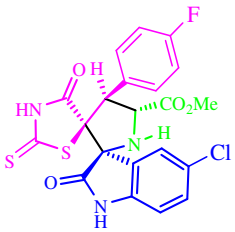

5o , 78%

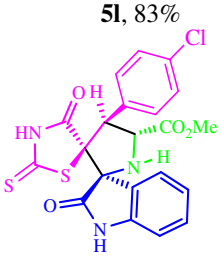

5p , 80%

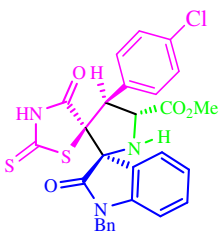

5q , 96%

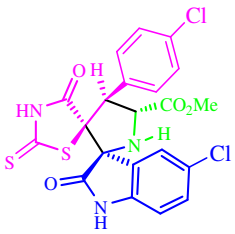

5r , 90%

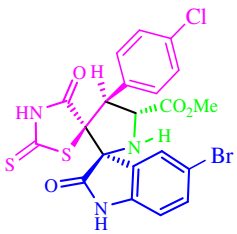

5s , 86%

[a] All reactions were carried out with **1** (1 mmol), **2** (1 mmol), **3** (1 mmol), NEt_3 (1 mmol) in CH_3CN (5.0 mL) at reflux for 2 h. Yields of the isolated cycloadducts are given.

The structure and the relative configuration of the isolated spiropyrrolidines **5a-s** were elucidated by analyzing their spectroscopic data (^{1}H NMR and ^{13}C NMR) and confirmed by an X-ray diffraction study performed on cycloadduct **5c**.

2.1.1. Spectroscopic and crystallographic characterization of the isomeric cycloadducts

The specific regioisomer was determined on the basis of the ^{1}H NMR chemical shifts of the H-4' and H-5' protons (Fig. 2). The ^{1}H NMR spectrum of **5g** shows two mutually coupled doublets at δ 4.39 ppm and 5.11 ppm with a ^3J coupling of 9.6 Hz, corresponding to the pyrrolidine ring and corroborating the formation of regioisomer **5g**. In the case of the hypothetical other regioisomer **6g** (Scheme 3), one would expect in the ^{1}H NMR spectrum the occurrence of two singlets for the pyrrolidinyl protons instead of two doublets. Furthermore, the methoxy protons give rise to a sharp singlet resonating 3.71 ppm. The aromatic protons found in the region between δ 6.82to 7.58 ppm appear as a multiplet. In addition, there are two broad singlets at δ 8.21 and δ 9.35 assigned to the NH protons of oxindole and rhodanine, respectively. The off-resonance decoupled ^{13}C-NMR spectrum of **5g** reveals the presence of two spiro carbons resonating at δ80.8 and 74.0 ppm, corresponding to C-2'and C-3', respectively (Fig.2). The two carbons C-4' and C-5' of the pyrrolidine ring are resonating at δ 64.8 and 60.8 ppm. In addition, the resonances at δ 176.7 ppm and δ 171.3 ppm are due to the oxindole and ester carbonyl groups, respectively. The signals at δ 178.2 ppm and δ197.2 ppm of **5g** are attributed to the ketonic carbonyl and thiocarbonyl carbons of rhodanine, respectively, corroborating further our structural proposal.

It is worth noting that in all cases, the reactions were found to be highly regioselective leading to the generation of only one regioisomer **5**. No indication for the copresence of isomer **6**, even in smaller amounts, was found (Scheme 2).

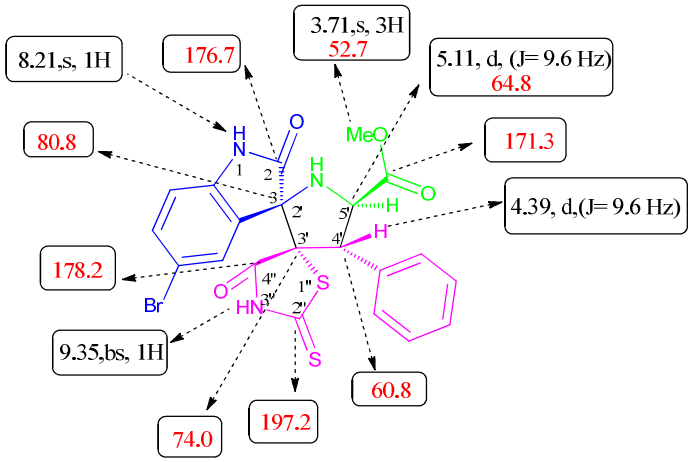

Fig. 2. Selected[1]H (black)and [13]C NMR (red) chemical shifts (ppm)of **5g**.

2.2.2. *Crystal structure determination of cycloadduct* ***5c***

The stereochemical outcome of the reaction was confirmed by single-crystal X-ray diffraction analysis of the cycloadduct **5c**. The molecular structure of **5c** is shown in Fig.3. Noteworthy, an intramolecular C–H1···O hydrogen bonding between H15 attached on the *p*-tolyl cycle and the O atom of the imide-type C27–O1 carbonyl function occurs. In the crystal, the individual molecules are associated through weak intermolecular N1–H1···O3[1], N3–H3···O3[2] bonding, giving rise to a supramolecular network (see Fig. S40 and Tables S1 and S2 in the SI). This structural characterization reveals that the cycloaddition reaction proceeds through an *exo*-transition state between the (*Z*)-5-arylidine-2-thioxothiazolidin-4-one and the *Z,E*-dipole affording only one diastereoisomer. Based on this finding, we suppose, also in line with the NMR data (see above), that the same plausible mechanism operates also for the other derivatives (see below) and that in consequence the stereochemistry of the other cycloadducts can be assigned by analogy.

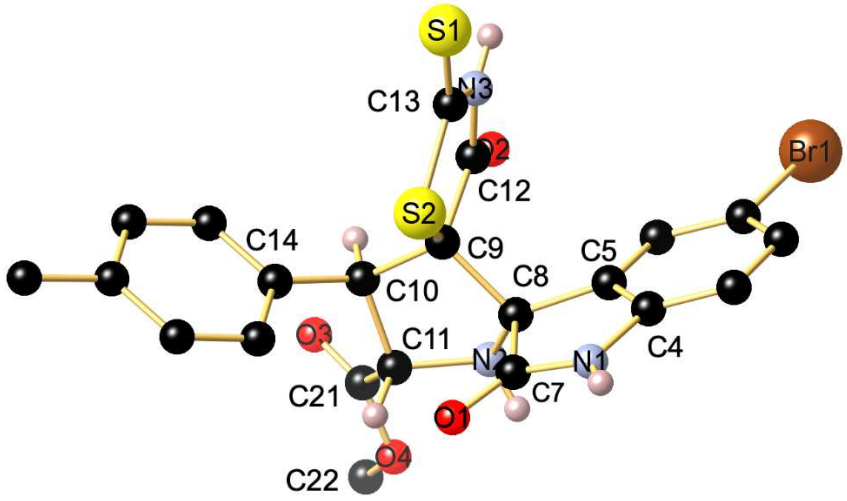

Fig. 3. Ball and sticks presentation of the molecular structure of **5c** recorded at 100 K. Only relevant H atoms are shown.

2.2.3. Discussion of the regio- and stereochemical route of the reaction

Based on the experimental results and similar previous reports [40-42], a plausible mechanism for the regio- and diasterioselective spiropyrrolidines formation represented in Scheme 4 can be proposed. The reaction proceeds through the generation of stabilized azomethine ylide **4** by condensation of isatin **2** with a primary amine **3** by thermal [1,5]-prototropy of the isatin-derived iminoester. The dipolarophile **1** undergoes then a subsequent 1,3-dipolar cycloaddition across the azomethine ylides, affording the desired products in a completely regio- and stereoselective manner. Four possible stereoisomers, related to two regioisomeric and two stereoisomeric approaches, might *à priori* be present in the thus formed spiro[pyrrolidine-3,2'-oxindoles] (Scheme 4). The cycloadducts were labelled *exo*-**5**, *endo*-**5**, *exo*-**6**, *endo*-**6** and their transition states (TS) TS-*exo*-**5**, TS-*endo*-**5**, TS-*exo*-**6** and TS-*endo*-**6**. As depicted in Scheme 3, a high regio- and diasterioselectivity was encountered in the formation of cycloadduct *exo*-**5**, which may be directed by the presence of stabilizing secondary orbital interactions (SOI) [43-45] between the oxygen atom of the carbonyl of the indole ring and the carbonyl carbon atom of the dipolarophile residue.

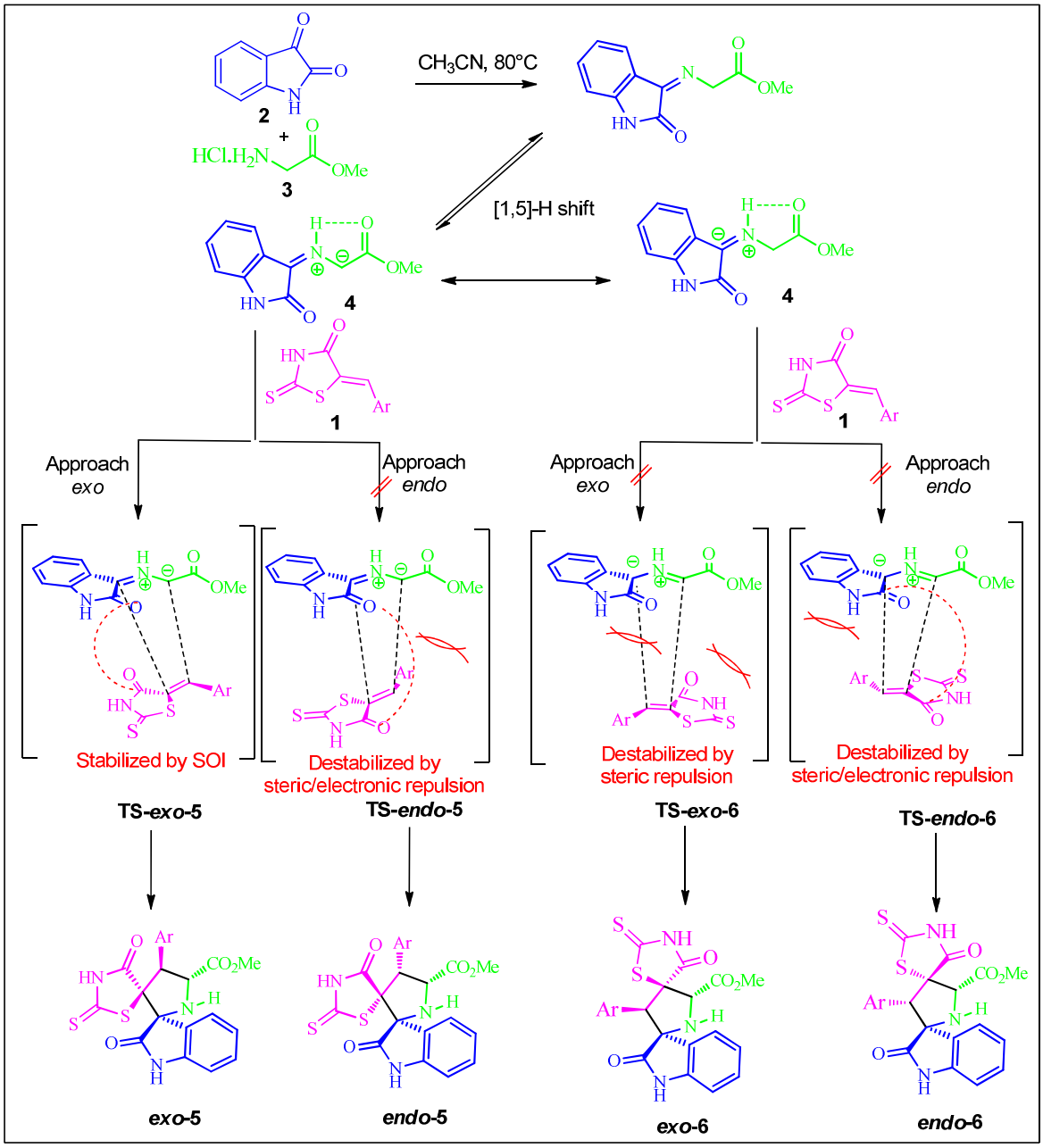

Scheme 3. Plausible mechanism for the regio- and stereoselective formation of spiropyrrolidines **5**.

The alternative possible transition states depicted in Scheme 3 appear to be less favorable due to steric crowding (TS-*exo*-**6**), and/or electronic repulsion occurred between the *cis* carbonyls of the arylidene and indole part, in case of TS-*endo*-**5** andTS-*endo*-**6**.

*2.3. In-vitro α-*amylase *inhibitory activity*

One of the therapeutic approaches for decreasing postprandial hyperglycaemia is to delay glucose absorption by the inhibition of the *α*-amylase activity [46,47]. Once in hand, the newly synthesized compounds were subjected to a preliminary evaluation of their *in vitro α*-amylase enzyme inhibition activity according to the standard method [48]. The anti-diabetic

drug Acarbose served as a standard in this investigation for comparison. The half maximal inhibitory concentration (IC_{50}) values of our compounds are reported in Table 3. We found that all compounds exhibit promising activities against *α*-amylase enzyme when used in µM concentration. It is notable that compounds **5g**, **5k**, and **5s** (IC_{50}, 1.49± 0.10, 1.50± 0.07, 1.57± 0.10 µM, respectively), followed by **5l**,**5q** and **5n**(IC_{50}, 1.59± 0.08, 1.63± 0.09and 1.67± 0.09 µM respectively) exhibited the highest inhibition potential, while **5c**, **5d** and **5j** showed moderate activity (IC_{50}, 1.72± 0.08, 1.73± 0.07, 1.75± 0.07 µM, respectively). Compounds **5a**, **5e** and **5f** (IC_{50}, 2.08± 0.11, 2.33± 0.13, 3.06± 0.17 µM, respectively) were the least active ones, but showed nevertheless satisfactory results in preliminary experiments, as compared to the hypoglycemic control drug acarbose (IC_{50}, 1.56± 0.07 µM) (Table 3).

Table 3. *In vitro α*-amylase inhibition assay of spiropyrrolidines **5**.

	Compound	Ar	R_1	R_2	IC_{50}(µM± SD)
1	**5a**	Me	H	H	2.08± 0.11
2	**5b**	Me	H	Bn	1.81± 0.09
3	**5c**	Me	Br	H	1.72± 0.08
4	**5d**	Me	Cl	H	1.73± 0.07
5	**5e**	H	H	H	2.33± 0.13
6	**5f**	H	Cl	H	3.06± 0.17
7	**5g**	H	Br	H	1.49± 0.10
8	**5h**	OMe	H	Bn	1.77± 0.08
9	**5i**	OMe	Br	H	1.97± 0.07
10	**5j**	Br	Cl	H	1.75± 0.07
11	**5k**	Br	Br	H	1.50± 0.07
12	**5l**	Br	NO_2	H	1.59± 0.08
13	**5m**	F	Br	H	Not tested
14	**5n**	F	H	Bn	1.67± 0.09
15	**5o**	F	Cl	H	2.00± 0.10
16	**5p**	Cl	H	H	1.83± 0.09
17	**5q**	Cl	H	Bn	1.63± 0.09
18	**5r**	Cl	Cl	H	1.97± 0.11
19	**5s**	Cl	Br	H	1.57± 0.10
20	**Acarbose**				1.56± 0.07

Mean value ± SD (n = 3).

2.4. Structure Activity Relationship – SAR.

It is evident that the inhibitory activity of the synthesized derivatives depends in a crucial manner on structural factors such as the nature of the substituents on the phenyl rings and the *N*-substituted group attached at the isatin core. As shown in Table 3, non-substituted

spiropyrrolidine **5e** (Ar= Ph, R_1= H, R_2= H) reveal a modest inhibition activity compared to the other compounds (IC_{50}= 2.33± 0.13µM). The incorporation of a bromo atom at the *p*-position of the isatin ring enhances extremely the inhibitory activity, rendering**5g** (Ar= Ph, R_1= Br, R_2= H) the most active compound (IC_{50}= 1.49± 0.10 µM). This result demonstrates further that the nature of the substituent on the phenyl ring of the isatin exerts a noticeable effect on the inhibition activity of spiropyrrolidine derivatives. The same improvement was noticed for series **5** derivatives incorporating a bromo-substituted isatin moiety such as **5k**, **5s**, **5c** and **5i** (Fig. 4). Double-halogenated compounds that contain also a *p*-halogen-substitution on the aromatic group of the dipolarophile (such as **5k** and **5s**) display somewhat superior activity compared to compounds **5c** and **5i**, the order of activity being (Br>Cl>Me>OMe). This difference of activity between all these derivatives may be explained by the inductive effect (-I) and the donor mesomeric effect (+M) of the *substituent* groups attached to the aromatic ring of the dipolarophile.

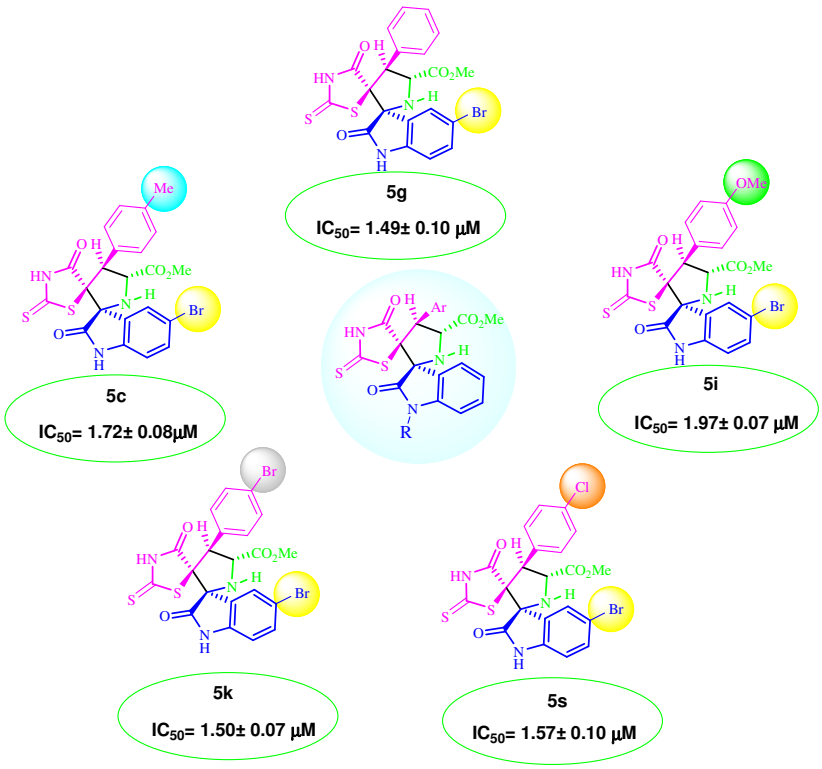

Fig. 4. Structure-activity relationship of compounds **5k**, **5s**, **5c**, **5i**, and **5g**.

This observation was evidenced from the screening of derivatives **5p**, **5a**and **5e** (Fig.5). Compound **5p** that is chloro-substituted on the aromatic group of the dipolarophile is among these latter three representatives still the most potent one (activity Cl>Me>H).

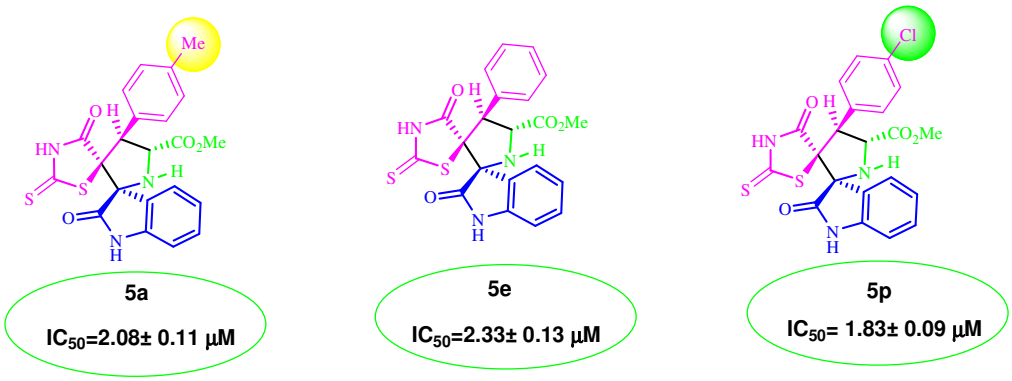

Fig. 5. Structure-activity relationship of compounds **5a**, **5e** and **5p**.

Interestingly, compounds of series **5** bearing a chloro-substituent on the isatin nucleus (Fig. 6), in particular compound **5d** bearing also a methyl group (Ar = *p*-$CH_3C_6H_4$, R_1= Cl, R_2= H), showed a superior activity compared to compounds **5j**, **5o**, **5r** and **5f**, the order of activity being Me> Br>Cl >F> H, respectively. In this case, the activity was considerably affected by introducing a methyl group at the 4-position of the aromatic cycle of the dipolarophile, most probably due to stronger interactions of **5d** with the active enzyme site.

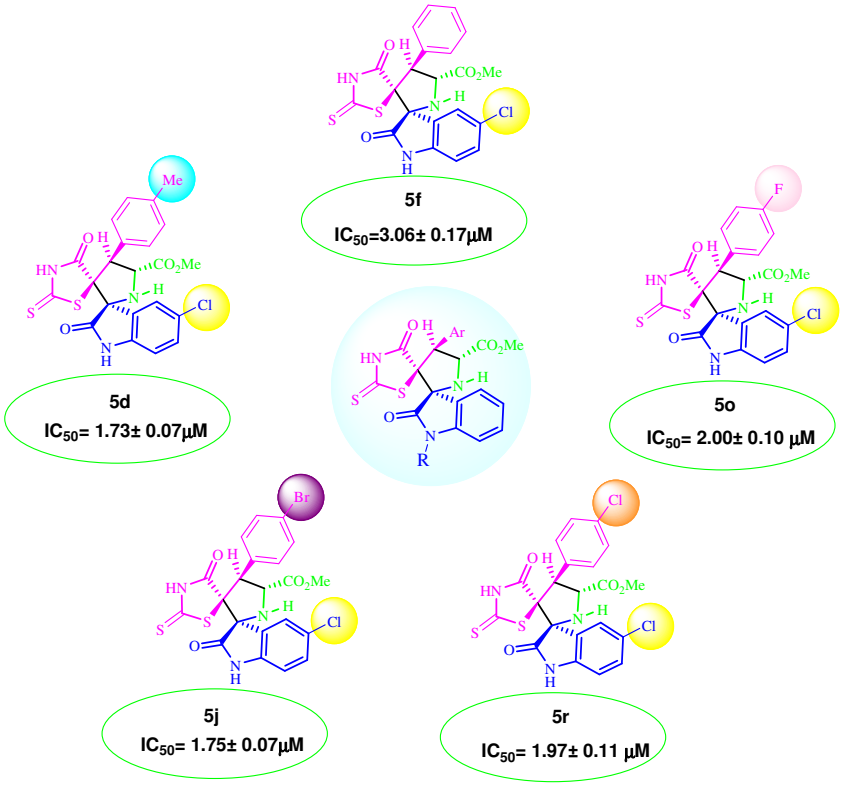

Fig. 6. Structure-activity relationship of compounds **5d**, **5j**, **5o**, **5r** and **5f**.

Furthermore, the incorporation of a benzyl group at the *N*-position of the isatin core causes a considerable increase in the α-amylase inhibition (Fig. 7). For instance, compound **5q** (Ar= *p*-

ClC_6H_4, R_1= H, R_2= Bn) is obviously more active than **5p** (Ar= *p*-ClC_6H_4, R_1= H, R_2= H). The *p*-halogen-substituted aryl derivatives of dipolarophile **5q** and **5n** also showed a better inhibitory activity in the order Cl> F> OMe> Me.

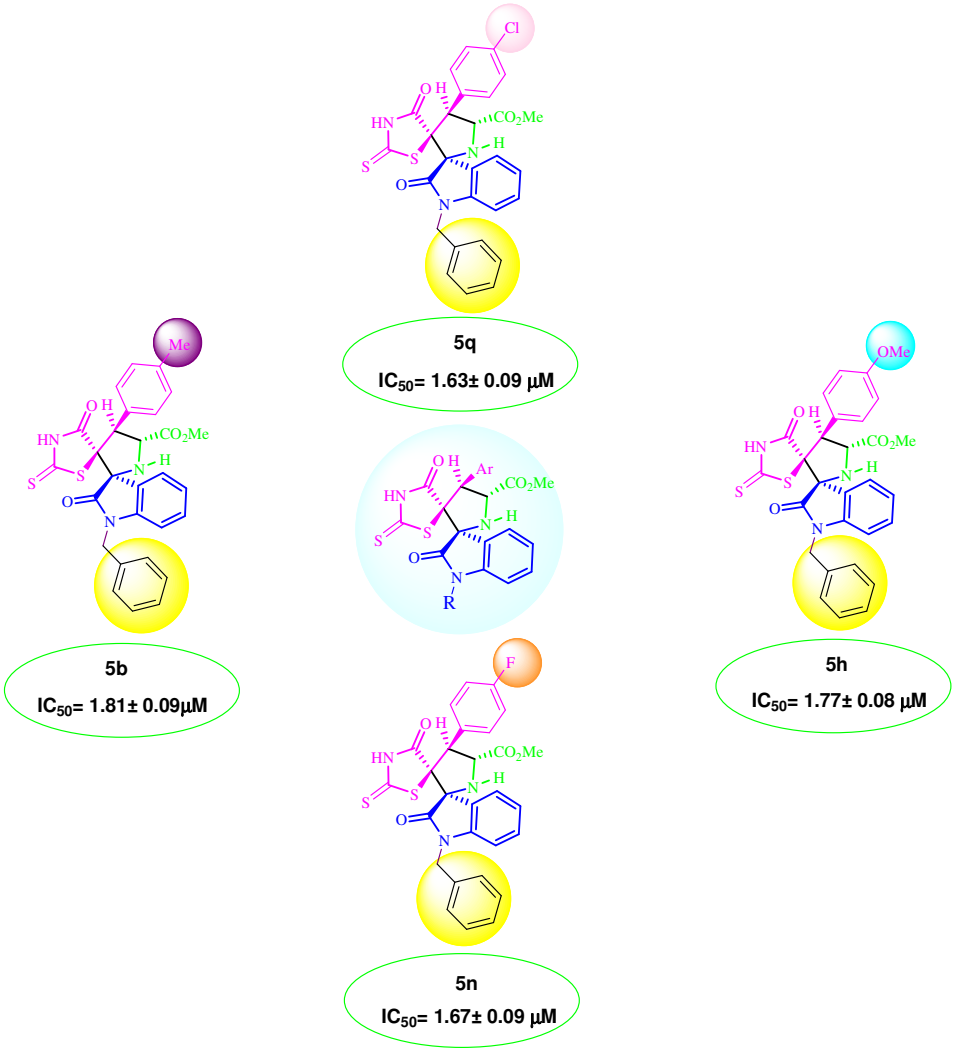

Fig. 7. Structure-activity relationship of compounds **5n**, **5q**, **5b** and **5h**.

Worth mentioning is also compound **5l** (IC_{50} = 1.59± 0.08 µM) (Table 3) bearing a *p*-nitro aryl cycle on the of isatin core, which displayed a good activity. This might be due to the electron-withdrawing nature of the NO_2 group. Limited inhibition activity of otherwise substituted spiropyrrolidine derivatives like **5f** suggest that the α-amylase inhibitory activity depends in a sensitive manner both on substitution on the dipolarophile and isatin core. In addition, compounds containing halogen substituents attached to the phenyl ring of *(Z)*-5-arylidine-2-thioxothiazolidin-4-ones exhibit generally a higher inhibitory potency against the amylase enzyme than derivatives incorporating an electron-donating group bonded to the same phenyl ring.

The inhibition potency of our heterocyclic systems may be compared favorably with those of other heterocycles compounds investigated by other research groups such as arylhydrazide-thiazolidinone derivatives (IC_{50} values ranging between 4.10 and 38.20µM as compared to the standard acarbose 1.70 µM) [49], thiazolidine-2,4-dione-pyrazole conjugates (IC_{50}= 4.08->200 µg/mL as compared to acarbose 8.0 µg/mL [50], or spirooxindoles and benzo[*b*]furan analogues (IC_{50}= 22.61-779.08 µM in comparison with acarbose 0.75 µM) [51].

2.5. Molecular docking studies

In order to get a deeper insight into the binding interactions of the spiropyrrolidine derivatives, molecular docking study of five selected compounds was performed against active site of pig pancreatic *α*-amylase. The docked compounds **5d**, **5g, 5k**, **5s** and **5p** fitted well in the binding site of the *α*-amylase and gave rise to different polar and non-polar interactions with the embedded amino acid residues, most importantly the ionic interaction between the protonated secondary cyclic amine group in the ligand and the carboxylate moiety of Asp300 and/or Glu233. Compound **5d** and **5g** showed the lowest binding energy reverberated by a docking score of -19.78 and - 18.45kcal/mol followed by **5k** and **5s** that showed comparable binding energies of -18.29 and -17.55 kcal/mol, and finally came compound **5p** with a docking score of -16.91 kcal/mol.

*2.5.1. Ligand interactions of compound **5d***

The molecular docking study of compound **5d** revealed various interactions with the binding site residues. The His305 residue showed a hydrogen bonding interaction with the negatively charged nitrogen of the thiazolidine ring, as shown in Fig. 8. The carbonyl groups of the thiazolidine and indoline rings are also able to hydrogen bonding with the His305 and Gly306 residues, respectively. Leu162 is involved in a σ-π-interaction with the π-system of the indole ring. Moreover, the protonated pyrrolidine nitrogen forms an ionic interaction (salt bridge) with the anionic carboxylate group of Asp300, which is an essential interaction afforded by the reference inhibitor acarbose. The chloro-substituent of the indoline ring can enter in contact with Val163. The positive electrostatic potential on the outer lobe of such a covalent bond could interact with electron cloud of the alkyl group of Val163. This noncovalent interaction might contribute greatly to the activity of the compound. In addition, the methyl group of the *p*-tolyl moiety does not seem to contribute to the binding since it is exposed to the exterior of the binding site and is not coming in contact to any of the amino acid residues lining the binding site of the enzyme.

*2.5.2. Ligand interactions of compound **5g** (the most potent inhibitor)*

His305 of active site residue forms hydrogen bonding interactions with the negatively charged nitrogen and the carbonyl group of the thiazolidine core. The π-system of the indole ring and the π-system of the 4'-phenyl cycle on the pyrolidine ring gives rise to a σ-π-interaction with the Leu162 and Trp59 residues, respectively. Furthermore, the protonated pyrrolidine nitrogen is involved in anionic interaction (salt bridge) with Asp300. The covalently bonded bromine atom at the indoline ring comes in contact with Val163. Again, the positive electrostatic potential on the outer lobe of this covalent bond could interact with the electron cloud of the alkyl group of Val163. As in the case of **5d**, this non-covalent interaction might contribute significantly to the inhibitory activity of this derivative (Fig. 8).

*2.5.3. Ligand interactions of compound **5k***

For the docked **5k** derivative, the negatively charged nitrogen and the carbonyl group of the thiazolidine ring interact through hydrogen bonding with His305. The π-system of the indole ring forms a σ-pi-interaction with Leu162. In addition, the protonated pyrrolidine nitrogen shows an ionic interaction (salt bridge) with the negatively charged carboxylate group of Asp300. The covalently bonded bromine atom of the indoline ring enters in contact with Val163. As in the previous cases, the positive electrostatic potential on the outer lobe of this covalent bond could interact with the electron cloud of the alkyl group of Val163. In contrast, the bromine atom at the *para*-position of the 4'-phenyl cycle on the pyrrolidine ring does not seem to contribute to the binding of the compound, since it is exposed to the exterior of the binding site and therefore not entering in contact to any of the amino acid residues lining the binding site of the enzyme (Fig. 8).

*2.5 4. Ligand interactions of compound **5s***

Compound **5s** displays two interactions, one hydrogen bonding between the negatively charged nitrogen and the carbonyl group of the thiazolidine ring with His305 and another σ-π-interaction between the π-system of the 4'-phenyl cycle with Val163 and Trp59. The protonated pyrrolidine nitrogen shows also an ionic interaction (salt bridge) with an anionic carboxylate function of Asp300. The covalently bonded bromine atom at the indoline ring comes in contact with Gly306. The positive electrostatic potential on the outer lobe of such covalent bond allows again an interaction with the electron cloud of the alkyl group of Gly306. The chloro-substituent at the *p*-position of the 4'-phenyl cycle attached on the pyrrolidine ring does not seem to contribute to the binding of the compound, as it is exposed

to the exterior of the binding site and is thus not coming in contact to any of the amino acid residues lining the binding site of the enzyme (Fig. 8).

2.5 4. Ligand interactions of compound ***5p***

The His305 residue was found to form a hydrogen bond interaction with the negatively charged nitrogen of the thiazolidine ring, while Asp300 interacts *via* hydrogen bonding with the protonated pyrrolidine nitrogen. Compound **5p** exhibits also an ionic interaction (salt bridge) between the protonated pyrrolidine nitrogen and the anionic carboxylate of Glu233. Moving the halogen atom from the indoline ring to the *p*-position of the 4'-phenyl on the pyrrolidine ring results in a diminished activity. In this case, the chlorine atom is situated outside the binding site and is therefore not in contact to any of the amino acid residues lining the active site of the enzyme. Accordingly, it was not able to form any kind of halogen interaction, which could be the reason behind the poor activity of the drug. It also forces to push the indoline ring a little bit outside the binding site, which in turn causes to lose the σ-π-interaction with Leu162. This feature could be another explanation for the lower activity of compound **5p** (Fig. 8).

Docking the reference inhibitor Acarbose using the same docking protocol showed that Acarbose iterated most of the amino acid interactions reported between the X-ray crystallized protein and the co-crystallized acarbose, such as Asp197, Val163, Trp59, and most importantly the polar interactions with the negatively charged Asp300 and Glu233 (Fig. 9). The binding energy was estimated to be -24.67 kcal/mol.

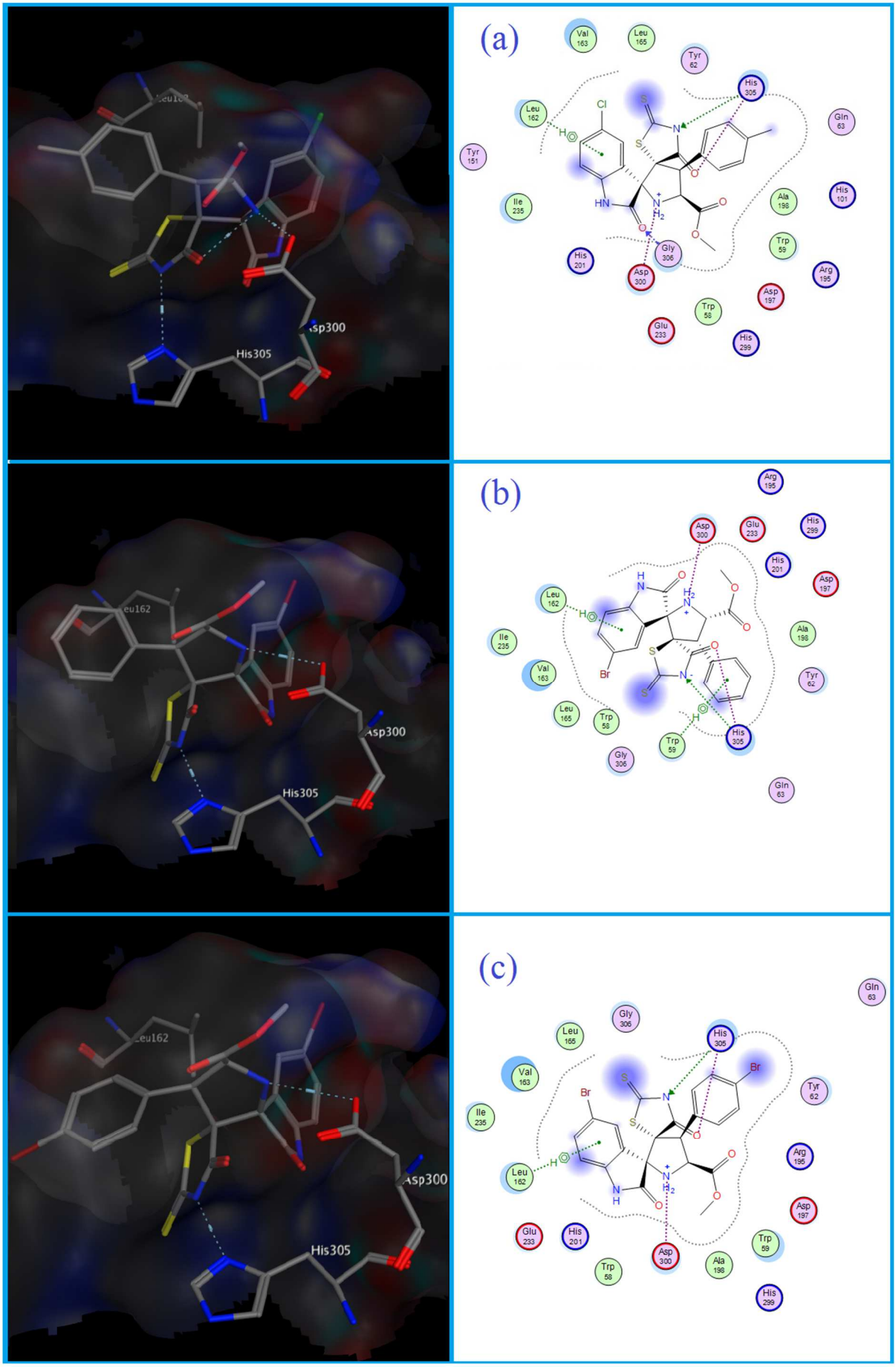
(a)
Val 163
Leu 165
Tyr 62
His 305
Leu 162
Gln 63
Tyr 151
His 101
Ile 235
Ala 198
Trp 59
His 201
Gly 306
Asp 300
Arg 195
Asp 197
Trp 58
Glu 233
His 299
sp300
His305
(b)
Arg 195
Asp 300
Glu 233
His 299
His 201
Asp 197
Leu 162
Ile 235
Ala 198
Val 163
Tyr 62
Leu 165
Trp 58
Trp 59
His 305
Gly 306
Gln 63
eu162
Asp300
His305
(c)
Gln 63
Gly 306
Leu 165
His 305
Val 163
Tyr 62
Ile 235
Arg 195
Leu 162
Asp 197
Glu 233
His 201
Trp 59
Asp 300
Ala 198
Trp 58
His 299
eu162
Asp300
His305

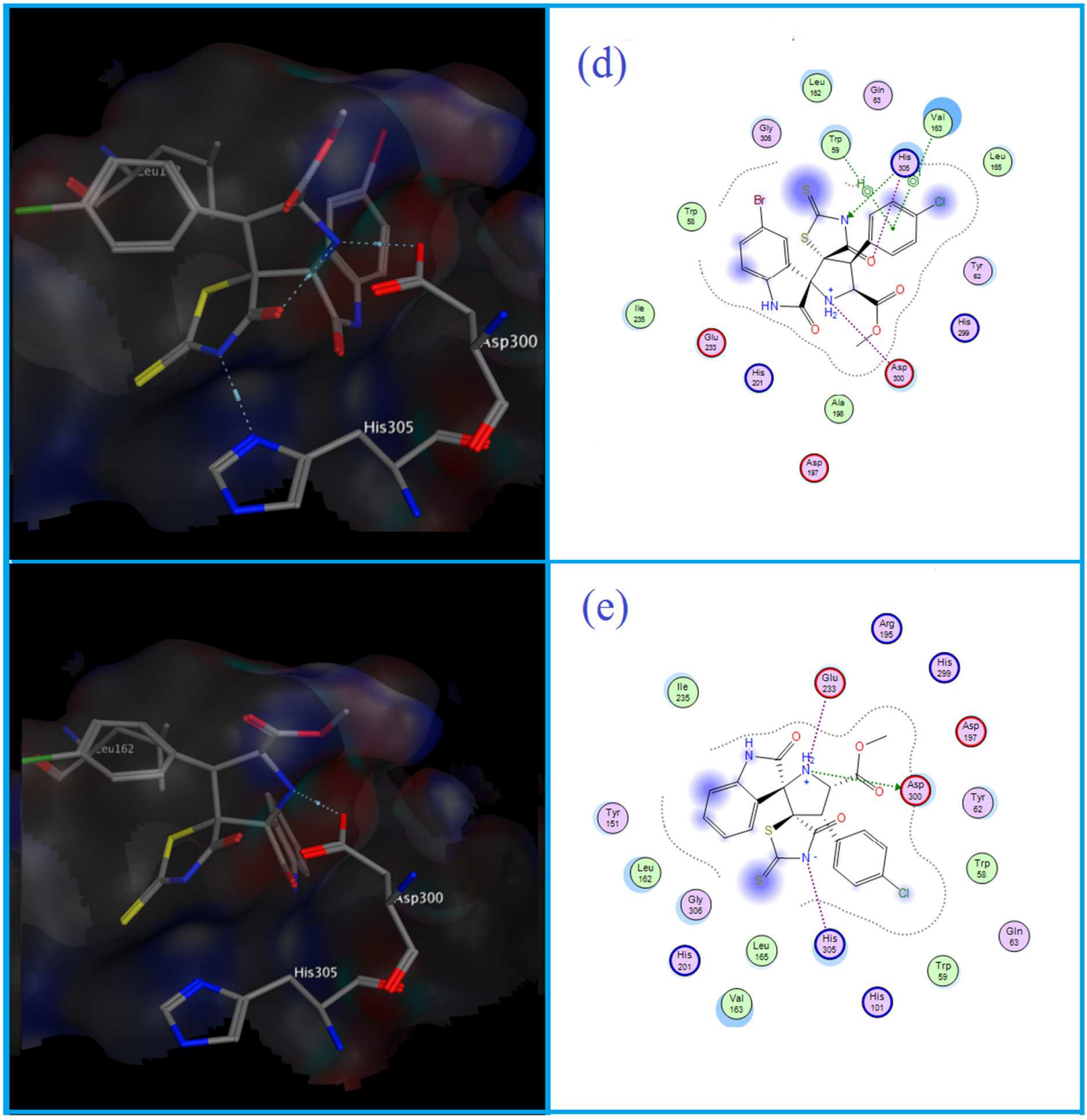

Fig. 8. Docking poses (2D, 3D) of compounds **5d**(a), **5g**(b), **5k**(c), **5s**(d) and **5p**(e) docked within the porcine *α*-amylase binding site.

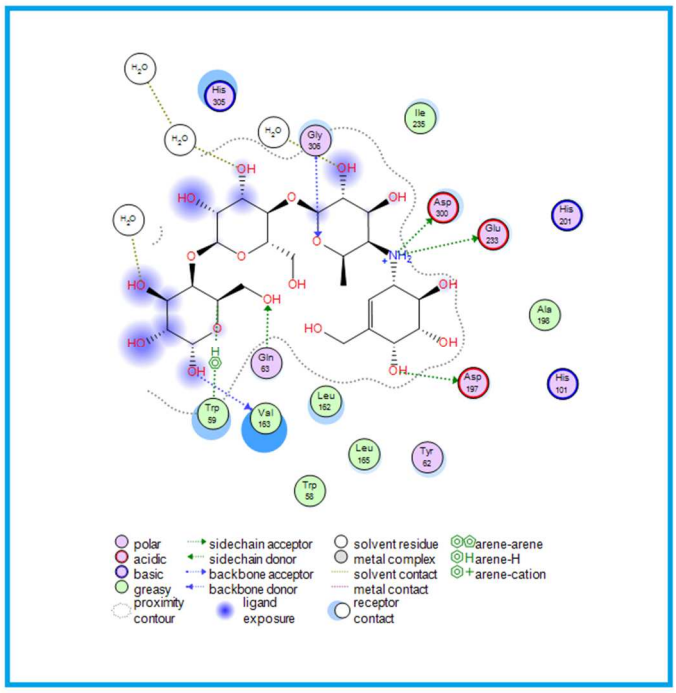

Fig. 9. Docking of the reference inhibitor acarbose at the porcine *α*-amylase binding site showing that it has iterated most of the reported amino acid interactions.

2.6. Anti-hyperglycemic effect of spiropyrrolidines ***5*** *on diabetic rats*

In vivo studies were carried out to evaluate the blood glucose lowering effect of our spiropyrrolidines in diabetic rats. As shown in Fig. 10, the blood glucose level increased significantly by 83% in the diabetic group (Group II) in comparison to normal rats (Group I). However, the daily administration of compounds **5g**, **5s**, **5k** and **5l** for one month to surviving diabetic rats was found to cause a significantly decrease of the serum glucose level by 6.8, 9.9, 12.3 and 5.5% respectively as compared to untreated diabetic rats.

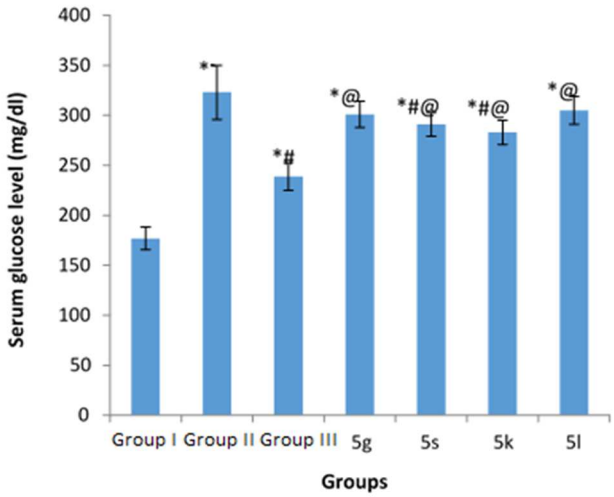

Fig. 10. Effect of spiropyrrolidines supplements on blood glucose level of diabetic rats. Values are given as mean ± SD for groups of 8 animals each. Values are statistically presented as follows: $^{*}P <$

0.05 significant differences compared to control group; $^{\#}P < 0.05$ significant differences compared to diabetic rats; $^{@}P < 0.05$ significant differences compared to acarbose-treated diabetic rats.

2.7. Oral glucose tolerance test in diabetic rats treated with spiropyrrolidines

The blood glucose levels were checked as per standard methods at 0, 30, 60, 90, 120 min intervals of the commencement of the experiment. The principal observation is that oral administration of all these heterocycles caused a significant decrease in blood glucose level as compared to the untreated diabetic control group. The blood glucose levels of **5g, 5s, 5k** and **5l** were lowered after 1h to 251, 269, 281 and 267 mg/dl, respectively, as compared to untreated diabetic rats (315 mg/dl) (Fig. 11). In fact, 1 hour after oral administration of **5g**, **5s**, **5k** and **5l** to diabetic rats, the blood glucose levels were lowered significantly by 20, 14.6, 10.7 and 15.2%. Therefore, these compounds deserve further exploration for the development of antidiabetic drugs with minimal side effects (Fig. 11).

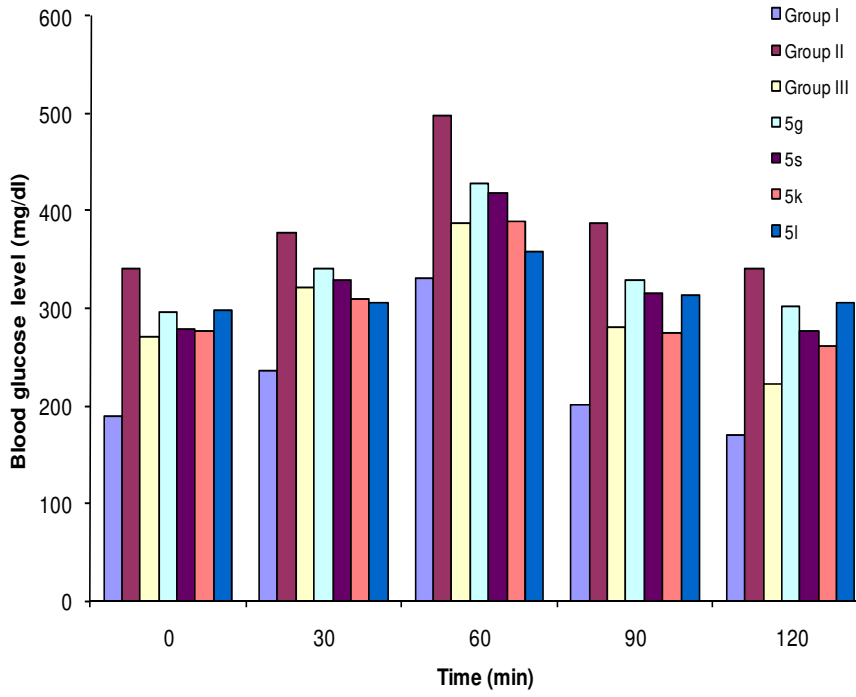

Fig. 11. Oral glucose tolerance test in diabetic rats treated with of spiropyrrolidines (**5g**, **5s**, **5k**, **5l**) and standard Acarbose. Group I: Normal rats with normal diet; Group II: diabetic control group; Group III: diabetic animals orally fed with acarbose at a dose of 10 mg/kg p.c daily by the gastric gavage method.

Conclusion

A three-component 1,3-dipolar cycloaddition of stabilized azomethine ylide generated *in situ* by the condensation of methyl glycine ester with isatin derivatives to various arylidene-rhodanines was developed affording a series of novel rhodanine-fused spiro[pyrrolidin-2,3'-oxindoles]. Screening all these derivatives *in vitro* against *α*-amylase enzyme, revealed that within series **5** the derivatives **5g**, **5k** and **5s** are the most active antidiabetic agents.

Limited structure–activity relationship (SAR) suggested that the nature and the electronic effect of the substituents present on the isatin moiety and the phenyl part of *(Z)*-5-arylidine-2-thioxothiazolidin-4-ones exert a significant influence on the inhibitory activity. It was noticed that substituted spiropyrrolidine derivatives exhibit a superior inhibitory activity than their unsubstituted congeners. This investigation furthermore evidences that compounds **5** bearing a halogen substituent on the phenyl rings feature a more potent inhibitory activity against α-amylase than derivatives bearing electron-donating groups.

Molecular docking study allowed to predict several important binding interactions of the spiropyrrolidine derivatives with the active site of *α*-amylase enzyme. Furthermore, an *in vivo* antidiabetic activity study using alloxan-induced diabetic rats indicated that compound **5k** presents significant hypoglycemic properties. Thus, these rhodanine-substitued spiropyrrolidine derivatives are valuable candidates deserving further exploration for future development of potential antidiabetic agents.

3. Experimental section

4.1. Materials and methods

^{1}H and ^{13}C NMR were recorded using a Bruker spectrometer operating at 400 and 100 MHz, respectively. The chemical shifts were recorded in ppm relative to tetramethylsilane and with the solvent resonance as the internal standard. Data were reported as follows: chemical shift, multiplicity (bs = broad singlet, s = singlet, d = doublet, dd = doublet of doublets, t = triplet, m = multiplet), coupling constants (Hz), integration. ^{13}C NMR data were collected with complete proton decoupling. Chemical shifts were reported in ppm with respect to TMS with the solvent resonance as internal standard. All chemicals were obtained from commercial sources and were used without further purification. Elemental analyses were performed on a Perkin Elmer 2400 Series II Elemental CHNS analyzer. Column chromatography was carried out on silica gel (300-400 mesh, Qingdao Marine Chemical Ltd., Qingdao, China). Thin layer

chromatography (TLC) was performed on TLC silica gel 60 F254 plates 0.2 mm 200x200 nm; The spots were visualized using UV light at 254 nm and 360 nm.

*3.2. General procedure for the synthesis of products **5a-s***

A mixture of *(Z)*-5-arylidine-2-thioxothiazolidin-4-ones **1**, (1 mmol), glycine methyl ester chloride **3** (1 mmol), and isatin **2**(1 mmol) in acetonitrile (5 mL) was stirred for 2h at 80 °C. After completion of the reaction (TLC), the solvent was removed under vacuum. The crude product was subjected to column chromatography on silica gel using cyclohexane/ethyl acetate (4:1 v/v) as eluent to give the pure products **5**.

*4.2.1. Methyl(3S,3'S,4'S,5'R)-4'-(p-tolyl)-2,4''-dioxo-2''-thioxodispiro[indoline-3,2'-pyrrolidine-3',5''-thiazolidine]-5'-carboxylate **5a**:*

pale yellow solid, Yield: 80%, Mp: 240-241°C, ^{1}H NMR δ (ppm) 2.38 (s, 3H, CH_3), 3.71 (s, 3H,OCH_3), 4.36 (d, *J*= 9.6 Hz, 1H, $H_{4'}$), 5.11 (d, *J*= 9.6 Hz, 1H,$H_{5'}$), 6.91 (t, *J*= 8 Hz, 1H, Ar-H), 7.10-7.20 (m, 3H, Ar-H), 7.22-723 (m, 2H, Ar-H), 7.31-7.45 (m, 2H, Ar-H), 8.89 (bs, 1H, NH); ^{13}C NMR δ 21.2, 52.6, 60.6, 64.7, 73.7, 79.5, 110.5, 119.0, 123.5, 124.0, 124.8, 129.9, 130.2, 130.7, 135.7, 141.5, 147.0, 152.1, 171.6, 176.7, 178.0, 201.3; Anal. Calcd. For $C_{22}H_{19}N_3O_4S_2$: C, 58.36; H, 4.22; N, 9.27; found: C, 58.46; H, 4.23; N, 9.30.

*4.2.2. Methyl(3S,3'S,4'S,5'R)-1-benzyl-4'-(p-tolyl)-2,4''-dioxo-2''-thioxodispiro-[indoline-3,2'-pyrrolidine-3',5''-thiazolidine]-5'-carboxylate **5b**:*

pale yellow solid, Yield: 95%, Mp: 218-219 °C, ^{1}H NMR δ (ppm) 2.36 (s, 3H, CH_3), 3.71 (s, 3H,OCH_3), 4.40 (d, *J*= 9.6 Hz, 1H,$H_{4'}$), 4.69 (d, *J*= 9.6 Hz, 1H,$H_{5'}$), 5.17-5.22 (m, 2H, $C\underline{H_2}$Bn), 6.67 (d, *J*= 8 Hz, 1H, Ar-H), 7.03-7.18 (m, 2H, Ar-H), 7.20-7.22 (m, 4H, Ar-H), 7.32-7.43(m, 6H, Ar-H), 8.61 (bs, 1H, NH); ^{13}C NMR δ 21.2, 43.8, 52.6, 60.6, 65.2, 73.9, 77.7, 110.1, 123.6, 125.3, 127.0, 127.3, 127.7, 128.9, 129.0, 129.4, 129.5, 129.7, 129.8, 130.2, 131.1, 133.2, 134.5, 138.1, 144.1, 171.6, 175.7, 178.3, 197.4; Anal. Calcd. For $C_{29}H_{25}N_3O_4S_2$: C, 64.07; H, 4.64; N, 7.73; found: C, 64.21; H, 4.62; N, 7.71.

*4.2.3. Methyl(3S,3'S,4'S,5'R)-5-bromo-2,4''-dioxo-2''-thioxo-4'-(p-tolyl)dispiro[indoline-3,2'-pyrrolidine-3',5''-thiazolidine]-5'-carboxylate **5c**:*

pale yellow solid, Yield: 86%, Mp: 197-198°C, ^{1}H NMR δ (ppm) 2.44 (s, 3H, CH_3), 3.72 (s, 3H, OCH_3), 4.35 (d, *J*= 9.6 Hz, 1H,$H_{4'}$), 5.08 (d, *J*= 9.6 Hz, 1H,$H_{5'}$), 6.55 (dd, *J*= 4 Hz, *J*= 8.4

Hz, 1H, Ar-H), 6.82 (d, *J*= 8.4 Hz,1H, Ar-H), 7.13-7.22 (m, 1H, Ar-H), 7.31-7.42 (m, 3H, Ar-H), 7.48-7.58 (m, 1H, Ar-H),8.00 (s, 1H, NH), 9.39 (bs, 1H, NH), ^{13}C NMR δ 21.3, 52.8, 60.7, 64.8, 74.0, 79.3, 112.1, 123.8, 128.5, 129.3, 129.7, 129.8, 130.2, 130.8, 133.8, 134.1, 138.5, 142.2, 171.2, 176.3, 178.2, 203.7; Anal. Calcd. For $C_{22}H_{18}BrN_3O_4S_2$: C, 49.63; H, 3.41; N, 7.89; found: C, 49.75; H, 3.39; N, 7.91.

4.2.4. Methyl(3S,3'S,4'S,5'R)-5-chloro-2,4''-dioxo-2''-thioxo-4'-(p-tolyl)dispiro[indoline-3,2'-pyrrolidine-3',5''-thiazolidine]-5'-carboxylate ***5d****:*

pale yellow solid, Yield: 83%, Mp: 221-222 °C, ^{1}H NMR δ (ppm) 2.38 (s, 3H, CH_3), 3.71(s, 3H, OCH_3), 4.36 (d, *J*= 9.6 Hz, 1H,$H_{4'}$), 5.11(d, *J*= 9.2 Hz, 1H,$H_{5'}$), 6.9 (d, *J*= 7.6 Hz, 1H, Ar-H), 7.10 (td, *J*= 1.2 Hz, *J*= 7.6 Hz, 1H, Ar-H), 7.21 (d, *J*= 8 Hz, 1H, Ar-H), 7.36-7.57 (m, 3H, Ar-H), 8.62 (bs, 1H, NH); ^{13}C NMR δ 21.3, 52.7, 60.7, 64.8, 74.1, 80.1, 111.1, 123.8, 128.1, 129.5, 129.6, 130.1, 131.3, 131.5, 133.4, 134.6, 138.1, 143.9, 171.9, 176.4, 177.7, 199.9; Anal. Calcd. For $C_{22}H_{18}ClN_3O_4S_2$: C, 54.15; H, 3.72; N, 8.61; found: C, 53.98; H, 3.70; N, 8.63.

4.2.5. Methyl(3S,3'S,4'S,5'R)-2,4''-dioxo-4'-phenyl-2''-thioxodispiro[indoline-3,2'-pyrrolidine-3',5''-thiazolidine]-5'-carboxylate ***5e****:*

pale yellow solid, Yield: 85%, Mp: 235-236°C, ^{1}H NMR δ (ppm) 3.71 (s, 3H, OCH_3), 4.39 (d, *J*= 9.6 Hz, 1H,$H_{4'}$), 5.14 (d, *J*= 9.6 Hz, 1H,$H_{5'}$), 6.92 (t, *J*= 8 Hz, 1H, Ar-H), 7.09 (t, *J*= 8 Hz, 1H, Ar-H),7.34-7.38 (m, 2H, Ar-H), 7.40-7.45 (m, 3H, Ar-H), 7.49-7.52 (m, 2H, Ar-H), 7.88 (s, 1H, NH), 9.09 (bs, 1H, NH); ^{13}C NMR δ 52.6, 60.9, 65.0, 74.7, 77.9, 110.6, 123.7, 125.9, 128.3, 129.1, 129.5, 129.9, 131.3, 133.5, 136.4, 138.8, 142.2, 171.5, 176.7, 178.3, 197.2; Anal. Calcd. For $C_{21}H_{17}N_3O_4S_2$: C, 57.39; H, 3.90; N, 9.56; found: C, 57.38; H, 3.91; N, 9.53.

4.2.6. Methyl(3S,3'S,4'S,5'R)-5-chloro-2,4''-dioxo-4'-phenyl-2''-thioxodispiro[indoline-3,2'-pyrrolidine-3',5''-thiazolidine]-5'-carboxylate ***5f****:*

pale yellow solid, Yield: 88%, Mp: 192-193°C, ^{1}H NMR δ (ppm) 3.71 (s, 3H, OCH_3), 4.39 (d, *J*= 9.6 Hz, 1H,$H_{4'}$), 5.12 (d, *J*= 9.2 Hz, 1H,$H_{5'}$), 6.88 (d, *J*= 8.4 Hz, 1H, Ar-H), 7.37-7.41 (m, 6H, Ar-H), 7.47-7.51 (m, 1H, Ar-H), 8.31 (s, 1H, NH), 9.58 (bs, 1H, NH); ^{13}C NMR δ 52.7, 60.8, 64.8, 74.2, 78.2, 111.7, 126.4, 128.4, 129.1, 129.4, 129.9, 130.6, 131.0, 131.3, 133.5, 135.9, 140.4, 171.3, 176.9, 178.2, 197.2; Anal. Calcd. For $C_{21}H_{16}ClN_3O_4S_2$: C, 53.22; H, 3.40; N, 8.87; found: C, 53.38; H, 3.39; N, 8.89.

4.2.7. Methyl(3S,3'S,4'S,5'R)-5-bromo-2,4''-dioxo-4'-phenyl-2''-thioxodispiro[indoline-3,2'-pyrrolidine-3',5''-thiazolidine]-5'-carboxylate ***5g****:*

pale yellow solid, Yield: 91%, Mp: 250-251 °C, ^{1}H NMR δ (ppm) 3.71 (s, 3H, OCH_3), 4.39 (d, *J*= 9.6 Hz, 1H,$H_{4'}$), 5.11 (d, *J*= 9.6 Hz, 1H,$H_{5'}$), 6.83 (d, J = 8 Hz, 1H, Ar-H), 7.33-7.42 (m, 3H, Ar-H), 7.46-7.51 (m, 3H, Ar-H), 7.58 (d, *J*= 2 Hz, 1H, Ar-H), 8.21 (s, 1H, NH),9.35 (bs, 1H, NH);^{13}C NMR δ 52.7, 60.8, 64.8, 74.0, 80.8, 112.2, 128.5, 128.7, 129.1, 129.4, 129.9, 130.6, 131.0, 133.5, 134.2, 135.9, 140.9, 171.3, 176.7, 178.2, 197.2; Anal. Calcd. For $C_{21}H_{16}BrN_3O_4S_2$: C, 48.65; H, 3.11; N, 8.11; found: C, 48.53; H, 3.10; N, 8.12.

4.2.8. Methyl(3S,3'S,4'S,5'R)-1-benzyl-4'-(p-methoxyphenyl)-2,4''-dioxo-2''-thioxodispiro-[indoline-3,2'-pyrrolidine-3',5''-thiazolidine]-5'-carboxylate ***5h****:*

pale yellow solid, Yield: 75%, Mp: 239-240 °C, ^{1}H NMR δ (ppm) 3.67 (s, 3H, OCH_3), 3.79 (s, 3H, OCH_3), 4.34 (d, *J*= 9.6 Hz, 1H,$H_{4'}$), 4.65 (d, *J*= 9.6 Hz, 1H,$H_{5'}$), 5.09-5.16 (m, 2H, $C\underline{H_2}$Bn), 6.62 (d, *J*= 7.6 Hz, 1H, Ar-H), 6.89 (d, *J*= 8.8 Hz, 2H, Ar-H), 7.00 (t, *J*= 7.6 Hz, 2H, Ar-H),7.19-7.31 (m, 5H, Ar-H), 7.39-7.42 (m, 3H, Ar-H), 8.70 (bs, 1H, NH); ^{13}C NMR δ 43.8, 52.6, 55.2, 60.4, 65.3, 73.4, 77.9, 110.1, 114.4, 123.1, 123.6, 125.4, 127.0, 127.7, 127.7, 128.2, 128.4, 128.8, 129.0, 130.4, 131.0, 131.2, 132.8, 134.5, 159.5, 171.6, 175.7, 178.3, 197.3; Anal. Calcd. For $C_{29}H_{25}N_3O_5S_2$: C, 62.24; H, 4.50; N, 7.51; found: C, 62.02; H, 4.51; N, 7.53.

4.2.9. methyl (3S,3'S,4'S,5'R)-5-bromo-2,4''-dioxo-2''-thioxo-4'-(p-methoxy)dispiro[indoline-3,2'-pyrrolidine-3',5''-thiazolidine]-5'-carboxylate ***5i****:*

pale yellow solid, Yield: 66%, Mp: 218-219 °C, ^{1}H NMR δ (ppm) 3.76 (s, 3H, OCH_3), 3.83 (s, 3H, OCH_3), 4.33 (d, *J*= 9.2 Hz, 1H,$H_{4'}$), 5.04 (d, *J*= 9.2 Hz, 1H,$H_{5'}$), 6.54 (dd, *J*= 5.7 Hz, *J*= 8.1 Hz, 1H, Ar-H), 6.81-6.92 (m, 1H, Ar-H), 7.02 (d, *J*= 8.4 Hz, 1H, Ar-H), 6.81-6.92 (m, 1H, Ar-H), 7.22-7.56 (m, 3H, Ar-H), 8.03 (s, 1H, NH), 10.14 (bs, 1H, NH);^{13}C NMR δ 52.7, 55.2, 60.1, 65.1, 73.6, 81.1, 114.0, 114.4, 115.0, 128.3, 128.9, 130.4, 131.1, 132.8, 133.0, 133.9, 139.6, 162.8, 171.3, 176.7, 178.4, 196.2; Anal. Calcd. For $C_{22}H_{18}Br\ N_3O_5S_2$: C, 48.18; H, 3.31; N, 7.66; found: C, 48.31; H, 3.30; N, 7.63.

4.2.10. Methyl(3S,3'S,4'S,5'R)-4'-(4-bromophenyl)-5-chloro-2,4''-dioxo-2''-thioxodispiro [indoline-3,2'-pyrrolidine-3',5''-thiazolidine]-5'-carboxylate ***5j****:*

pale yellow solid, Yield: 81%, Mp: 186-187 °C, ^{1}H NMR δ (ppm) 3.73 (s, 3H, OCH_3), 4.33 (d, *J*= 9.5 Hz, 1H,$H_{4'}$), 5.04 (d, *J*= 9.5 Hz, 1H,$H_{5'}$), 6.87(d, *J* = 8.1 Hz, 1H, Ar-H), 7.37 (dd, *J*

= 8.3 Hz, *J* = 6.3 Hz, 2H, Ar-H), 7.55 (d, *J* = 8.4 Hz, 2H, Ar-H), 7.67 – 7.59 (m, 2H, Ar-H), 9.04 (s, 1H, NH), 9.71 (s, 1H, NH) ; ^{13}C NMR δ 52.4, 60.1, 65.0, 74.1, 77.8, 111.6, 122.6, 124.8, 125.7, 126.4, 129.0, 131.6, 131.8, 132.3, 132.7, 135.1, 140.1, 171.0, 176.3, 177.8, 197.1; Anal. Calcd. For $C_{21}H_{15}BrClN_3O_4S_2$: C, 45.62; H, 2.73; N, 7.60; found: C, 45.61; H, 2.74; N, 7.61.

4.2.11. Methyl(3S,3'S,4'S,5'R)-5-bromo-2,4''-dioxo-2''-thioxo-4'-(p-bromophenyl)dispiro-[indoline-3,2'-pyrrolidine-3',5''-thiazolidine]-5'-carboxylate ***5k****:*

pale yellow solid, Yield: 85%, Mp: 226- 227 °C, ^{1}H NMR δ (ppm) 3.73 (m, 3H, OCH_3), 4.33 (d, *J*= 9.6 Hz, 1H,$H_{4'}$), 5.04 (d, *J*= 9.6 Hz, 1H,$H_{5'}$), 6.87 (d, *J*= 8.4 Hz, 1H, Ar-H), 7.19-7.24 (m, 1H, Ar-H), 7.34-7.39 (m, 2H, Ar-H), 7.44-7.56 (m, 3H, Ar-H), 8.70 (bs, 1H, NH); ^{13}C NMR δ 52.5, 60.1, 64.8, 74.0, 80.4, 111.5, 122.9, 126.1, 129.0, 131.2, 131.4, 131.8, 131.9, 132.3, 132.7, 135.7, 140.2, 171.0, 176.2, 177.4, 196.5; Anal. Calcd. For $C_{21}H_{15}Br_2N_3O_4S_2$: C, 42.23; H, 2.53; N, 7.04; found: C, 42.36; H, 2.54; N, 7.02.

*4.2.12. Methyl(3S,3'S,4'S,5'R)-4'-(4-bromophenyl)-5-nitro-2,4''-dioxo-2''-thioxodispiro-[indoline-3,2'-pyrrolidine-3',5''-thiazolidine]-5'-carboxylate****5l****:*

pale yellow solid, Yield: 83%, Mp: 210- 211 °C, ^{1}H NMR δ (ppm) 3.85 (s, 3H, OCH_3), 4.28 (d, *J*= 9.6 Hz, 1H,$H_{4'}$), 5.01 (d, *J*= 9.6 Hz, 1H,$H_{5'}$), 6.69 (d, *J*= 9.2 Hz, 1H, Ar-H), 6.75-6.79 (m, 1H, Ar-H), 7.36 (d, *J*= 8.4 Hz, 1H, Ar-H), 7.60-7.66 (m, 1H, Ar-H), 8.13 (dd, *J*= 2.4 Hz, *J*= 9.2 Hz, 1H, Ar-H), 8.45 (d, *J*= 2.4, 1H, Ar-H), 9.48 (bs, 1H, NH) ; ^{13}C NMR δ 52.8, 61.7, 64.7, 73.6, 81.2, 115.9, 124.5, 124.8, 125.5, 126.5, 127.5, 128.3, 131.3, 132.0, 132.6, 138.1, 141.2, 171.3, 176.0, 177.7, 200.2; Anal. Calcd. For $C_{21}H_{15}BrN_4O_6S_2$: C, 44.77; H, 2.68; N, 9.94; found: C, 44.66; H, 2.69; N, 9.95.

4.2.13. Methyl(3S,3'S,4'S,5'R)-5-bromo-2,4''-dioxo-2''-thioxo-4'-(p-fluorophenyl)dispiro [indoline-3,2'-pyrrolidine-3',5''-thiazolidine]-5'-carboxylate ***5m:***

pale yellow solid, Yield: 84%, Mp: 225-226 °C, ^{1}H NMR δ (ppm) 3.73 (s, 3H, OCH_3), 4.37 (d, *J*= 9.6 Hz, 1H,$H_{4'}$), 5.05 (d, *J*= 9.6 Hz, 1H,$H_{5'}$), 6.83 (d, *J*= 8.4 Hz, 1H, Ar-H), 7.10 (t, *J*= 8.4 Hz, 2H, Ar-H), 7.46-7.51 (m, 3H, Ar-H), 7.58 (t, *J*= 1.6 Hz, 1H, Ar-H), 8.19 (s, 1H, NH), 9.40 (s, 1H, NH); ^{13}C NMR δ 52.8, 60.0, 65.0, 74.2, 80.8, 112.2, 116.2, 116.7, 125.4, 129.1, 131.6, 131,9 , 132.7, 134.3, 140.8, 171.1, 176.7, 178.3, 197.0; Anal. Calcd. For $C_{21}H_{15}BrFN_3O_4S_2$: C, 47.17; H, 2.83; N, 7.83; found: C, 47.02; H, 2.82; N, 7.62.

4.2.14. Methyl(3S,3'S,4'S,5'R)-1-benzyl-4'-(p-fluorophenyl)-2,4''-dioxo-2''-thioxodispiro-[indoline-3,2'-pyrrolidine-3',5''-thiazolidine]-5'-carboxylate ***5n:***

pale yellow solid, Yield: 94%, Mp: 247-248 °C, ^{1}H NMR δ (ppm) 3.69 (s, 3H, OCH_3), 4.36 (d, *J*= 9.6 Hz, 1H, $H_{4'}$), 4.66 (d, *J*= 9.6 Hz, 1H, $H_{5'}$), 5.10-5.15 (m, 2H, C$\underline{H_2}$Bn), 6.64 (d, *J*= 8 Hz, Ar-H), 7.01 (t, *J*= 8 Hz, 1H, Ar-H), 7.20-7.25 (m, 3H, Ar-H), 7.30-7.40 (m, 7H, Ar-H), 7.44-7.46 (m, 1H, Ar-H), 8.97 (bs, 1H, NH);^{13}C NMR δ 43.8, 52.7, 60.3, 65.3, 74.2, 80.2, 110.4, 114.0, 123.6, 123.8, 126.4, 127.0, 127.8, 128.4, 128.5, 128.8, 129.0, 130.5, 131.0, 132.3, 134.5, 144.2, 171.2, 175.6, 178.2, 196.7; Anal. Calcd. For $C_{28}H_{22}FN_3O_4S_2$: C, 61.41; H, 4.05; N, 7.67; found: C, 61.50; H, 4.06; N, 7.66.

4.2.15. Methyl(3S,3'S,4'S,5'R)-5-chloro-2,4''-dioxo-2''-thioxo-4'-(p-fluorophenyl)dispiro-[indoline-3,2'-pyrrolidine-3',5''-thiazolidine]-5'-carboxylate ***5o:***

pale yellow solid, Yield: 78%, Mp: 245- 247 °C, ^{1}H NMR δ (ppm) 3.73 (s, 3H, OCH_3), 4.36 (d, *J*= 9.6 Hz, 1H, $H_{4'}$), 5.05 (d, *J*= 9.6 Hz, 1H, $H_{5'}$), 6.87 (d, *J*= 8.4 Hz, 1H, Ar-H), 7.10 (t, *J*= 8.8 Hz, 2H, Ar-H), 7.36 (m, 1H, Ar-H), 7.44-7.49 (m, 3H, Ar-H),8.97 (s, 1H, NH); ^{13}C NMR δ ^{13}C NMR ($CDCl_3$, 100 MHz) δ 52.8, 60.3, 64.7, 74.2, 79.4, 111.6, 116.3, 125.6, 126.3, 128.5, 129.1, 131.4, 131.5, 132.0, 132.7, 134.8, 141.9, 171.3, 176.7, 178.2, 196.5; Anal. Calcd. For $C_{21}H_{15}ClFN_3O_4S_2$: C, 51.27; H, 3.07; N, 8.54; found: C, 51.35; H, 3.08; N, 8.51.

4.2.16. Methyl(3S,3'S,4'S,5'R)-4'-(p-chlolorophenyl)-2,4''-dioxo-2''-thioxodispiro[indoline-3,2'-pyrrolidine-3',5''-thiazolidine]-5'-carboxylate ***5p:***

white solid, Yield: 80%, Mp: 221- 222 °C, ^{1}H NMR δ (ppm) 3.72 (s, 3H, OCH_3), 4.35 (d, *J*= 9.2 Hz, 1H, $H_{4'}$), 5.07 (d, *J*= 9.2 Hz, 1H, $H_{5'}$), 6.92 (d, *J*= 8 Hz, 1H, Ar-H), 7.37-7.44 (m, 7H, Ar-H), 8.08 (s, 1H, NH), 9.27 (bs, 1H, NH); ^{13}C NMR δ 52.7, 60.2, 65.1, 74.3, 81.8, 110.5, 112.2, 123.7, 124.0, 125.7, 129.3, 129.8, 131.3, 131.4, 134.7, 138.8, 141.6, 171.3, 176.9, 178.4, 197.2; Anal. Calcd. For $C_{21}H_{16}ClN_3O_4S_2$: C, 53.22; H, 3.40; N, 8.87; found: C, 53.08; H, 3.41; N, 8.89.

4.2.17. Methyl(3S,3'S,4'S,5'R)-1-benzyl-4'-(p-Chlorophenyl)-2,4''-dioxo-2''-thioxodispiro-[indoline-3,2'-pyrrolidine-3',5''-thiazolidine]-5'-carboxylate ***5q:***

yellow solid, Yield: 96%, Mp: 166- 167 °C, ^{1}H NMR δ (ppm) 3.68 (s, 3H, OCH_3), 4.34 (d, *J*= 9.6 Hz, 1H, $H_{4'}$), 4.66 (d, *J*= 9.6 Hz, 1H, $H_{5'}$), 5.09-5.15 (m, 2H,, C$\underline{H_2}$Bn), 6.64 (d, *J*= 8 Hz, 1H, Ar-H), 7.03 (t, *J*= 8 Hz, 1H, Ar-H), 7.22-7.24 (m, 5H, Ar-H), 7.29-7.40 (m, 5H, Ar-H), 7.45 (m, 1H, Ar-H), 8.96 (bs, 1H, NH); ^{13}C NMR δ 43.8 52.7, 60.1, 65.3, 74.0, 80.2, 110.2,

122.8, 123.7, 125.3, 127.0, 127.8, 129.1, 129.3, 131.3, 131.3, 134.4, 134.4, 134.9, 144.0, 171.3, 175.7, 178.2, 196.8; Anal. Calcd. For $C_{28}H_{22}ClN_3O_4S_2$: C, 59.62; H, 3.93; N, 7.45; found: C, 59.71; H, 3.91; N, 7.47.

4.2.18. Methyl(3S,3'S,4'S,5'R)-5-chloro-2,4''-dioxo-2''-thioxo-4'-(p-chlorophenyl)dispiro-[indoline-3,2'-pyrrolidine-3',5''-thiazolidine]-5'-carboxylate ***5r:***

pale yellow solid, Yield: 90%, Mp: 216-217 °C, ^{1}H NMR δ (ppm) 3.73 (s, 3H, OCH_3), 4.34 (d, *J*= 9.2 Hz, 1H, $H_{4'}$), 4.04 (d, *J*= 9.2 Hz, 1H, $H_{5'}$), 6.87 (d, *J*= 8.4 Hz, 1H, Ar-H), 7.36-7.40 (m, 3H,Ar-H), 7.43-7.48 (m, 3H, Ar-H), 8.16 (bs, 1H, NH), 9.03 (bs, 1H, NH); ^{13}C NMR ($CDCl_3$, 100 MHz) δ ^{13}C NMR δ 52.8, 60.2, 64.9, 74.2, 82.0, 111.8, 125.7, 126.4, 129.3, 129.8, 131.3, 131.4, 131.7, 131.9, 134.5, 138.1, 140.3, 170.9, 176.4, 178.1, 197.3; Anal. Calcd. For $C_{21}H_{15}Cl_2N_3O_4S_2$: C, 49.61; H, 2.97; N, 8.27; found: C, 49.66; H, 2.96; N, 8.30.

4.2.19. Methyl(3S,3'S,4'S,5'R)-5-bromo-2,4''-dioxo-2''-thioxo-4'-(p-chlorophenyl)dispiro-[indoline-3,2'-pyrrolidine-3',5''-thiazolidine]-5'-carboxylate ***5s:***

pale yellow solid, Yield: 86%, Mp: 251- 252 °C, ^{1}H NMR δ (ppm) 3.73 (s, 3H, OCH_3), 4.34 (d, *J*= 9.6 Hz, 1H, $H_{4'}$), 5.02 (d, *J*= 9.6 Hz, 1H, $H_{5'}$), 6.82 (d, *J*= 8.4 Hz, 1H,Ar-H), 7.34-7.40 (m, 2H,Ar-H), 7.45-7.58 (m, 3H,Ar-H), 7.57 (d, *J*= 1.6 Hz, 1H,Ar-H), 8.28 (bs, 1H, NH), 9.42 (bs, 1H, NH); ^{13}C NMR δ 52.7, 60.0, 65.1, 73.0, 81.2, 114.9, 124.8, 125.8, 128.1, 129.0, 129.1, 129.9, 130.5, 131.6, 131.9, 137.4, 140.8, 171.3, 176.4, 177.4, 195.5; Anal. Calcd. For $C_{21}H_{15}BrClN_3O_4S_2$: C, 45.62; H, 2.73; N, 7.60; found: C, 45.63; H, 2.72; N, 7.58.

3.3. X-Ray crystal structure analysis of compound ***5c***

Colorless X-ray-suitable crystals of **5c** were grown by recrystallization from EtOH.$C_{22}H_{18}BrN_3O_4S_2$: M = 532.42, monoclinic, space group $P2_1/n$, a = 10.3333(4) Å, b = 17.3788(7) Å, c = 12.7619(5) Å, β = 109.6620(10)°, V = 2158.16(15) Å^3, Z = 4, D_c = 1.639 g/cm^3, λ(Mo-Kα) = 0.71073 Å, F(000) = 1080, μ/mm^{-1}= 2.135, T = 100(2) K. 50223 reflections collected, 9491independent with $I>2\sigma(I)$. Final residuals ρ_{max} = 0.84, ρ_{min} = -0.163 e$^-$/Å^3. Final agreement factors: $R(F)$ = 0.0275 and 0.0351, $wR(F2)$ = 0.0677 and 0.0714 for $I>2\sigma(I)$ and all data, respectively, GOF = 1.027.

The crystal structure determination was accomplished on a *Bruker D8 Venture* four-circle diffractometer using a *PHOTON II* CPAD detector by *Bruker AXS GmbH*. X-ray radiation was generated by microfocus source *IμS* Mo (λ□□ 0.71073Å) from *Incoatec GmbH* with HELIOS mirror optics and a single-hole collimator from *Bruker AXS GmbH*. A suitable

crystal of **5c** was covered with an inert oil (perfluoropolyalkylether) and mounted on a *MicroMount*from *MiTeGen*. For the data collection, the programs APEX 3 Suite (v.2018.7-2) with the integrated programs SAINT (integration) and SADABS (adsorption correction) by *Bruker AXS GmbH* were used. The processing and finalization of the crystal structure was done with the program Olex2[52]. The crystal structure was solved with the ShelXT [53] structure solution program using Intrinsic Phasing and refined with the ShelXL [54] refinement package using Least Squares minimization. The non-hydrogen atoms were refined anisotropically. The C-bound H atoms were placed in geometrically calculated positions and each was assigned a fixed isotropic displacement parameter based on a riding-model: C–H = 0.95–1.00 Å with U_{iso}(H) = 1.5U_{eq}(CH_3) and 1.2U_{eq}(CH) for other hydrogen atoms. The *N*-bound hydrogen atoms were located in the difference-Fourier-map and refined independently. Crystallographic data for the structure of **5c** have been deposited with the Cambridge Crystallographic Data Centre as supplementary publication number 1994835. Copy of these data can be obtained, free of charge, on application to CCDC, 12 Union Road, Cambridge CB2 IEZ, UK, fax: 144-(0)1223-336033 or e-mail: deposit@ccdc.cam.ac.uk.

3.4. Experimental method for the in vitro α-amylase assay

The *in vitro* α-amylase inhibition activity of all drugs was determined based on the spectrophotometric assay using acarbose as the reference compound. The heterocycles 5 were dissolved in DMSO to give concentrations ranging from 1, 4, 8 and 16 mg/mL. Appropriate dilutions (1–16 mg/mL) of the heterocycles **5** and 500 µl of 0.02 M sodium phosphate buffer (pH 6.9 with 0.006 M NaCl) containing porcine pancreatic α-amylase (EC 3.2.1.1) (0.5 mg/mL) were incubated at 25°C for 10 min. Then, 500 µl of 1% starch solution in 0.02 M sodium phosphate buffer (pH 6.9 with 0.006 M NaCl) was added to the reacting mixture. After that, 1.0 mL of dinitrosalicylic acid (DNSA) was added to the mixture which was incubated at 37 °C for 5 min. The reaction was stopped by incubating in a boiling water bath for 5 min and subsequent cooling to room temperature. The absorbance was measured at 540 nm. The α-amylase inhibitory activity was expressed as percentage inhibition [55].

$$\text{Inhibition } (\%) = [(Abs_{ref} - Abs_{sample})/=Abs_{ref}]* 100$$

3.5. Experimental induction of diabetes

The assays of the present study were conducted on adult male *Wistar* rats, weighing 170 ± 10 g, which were obtained from the local Central Pharmacy, Tunisia. All rats were kept in an environmentally controlled breeding room (temperature: 24 ± 2°C, humidity: 60 ± 5%, 12-h dark/light cycle) where they had standard diets and free access to tap water. The animal studies conducted in this work followed the International Guidelines for Animal Care Directive 86/609/EEC, and was approved by the Tunisian Ethics Committee of the University of Monastir (Monastir, Tunisia) for the care and use of laboratory animals.

Diabetes was induced in rats by a single intraperitoneal injection of freshly prepared alloxan solution in normal saline at a dose of 150 mg/kg body weight [55]. After three days, the rats whose blood glucose was higher 280 mg/dl were chosen for the experiment. The rats were divided into eight groups of eight animals, each as follows: Group I: normal animal; Group II: untreated diabetic rats; Group III: diabetic animals treated with standard drug as acarbose at a dose of 10 mg/kg; and Group IV: the diabetic rats treated with the spiropyrrolidine derivatives at a dose of 20 mg/kg. The spiropyrrolidine derivatives and acarbose were dissolved in DMSO at a concertation of 4% in water. All groups of rats were given a dose of DMSO of 4% in water by gastric gavage route to standardize the conditions of the experiment. One month later and 12 h after last feeding, the rats were sacrificed by decapitation, and their trunk blood collected. The serum was prepared by centrifugation (1,500 ×g, 15 min, 4°C). The serum glucose level was measured by measuring the amount of red quinoneimine released from oxidation of glucose substrate (Kits, Biolabo, France, ref 80009).

For oral glucose tolerance test (OGTT), 8 normal and 36 surviving diabetic rats obtained 3 days after alloxan injection were used. Rats of the experimental groups received 20 mg/kg of the test substances or acarbose in 4% DMSO by gastric gavage route. After 30 min, all animals were administered intragastrically with 2 g/kg sucrose in 0.9% sodium chloride solution. Blood glucose levels of all rats were tested initially before the glucose administration and 0, 30, 60, 90 and 120 min of post-glucose administration [56,57].

3.6. Docking protocol

The X-ray crystallographic structure of the procine α-amylase in complex with acarbose (PDB code: 1OSE) was downloaded from the protein data bank (www.rcsb.org). The docking protocol was applied using Molecular Operating Environment (2010.10; Chemical Computing Group Inc., Montreal, Canada) software. The downloaded protein was protonated to add the hydrogen atoms that were not detected during the crystallization process. Compounds selected

for docking were drawn using MOE builder tool. The compounds were then washed to set their ionization state. The MMFF94x force field was used to compute the energy minimization for the compounds. Docking was done applying the default settings of placement and scoring [58].

Appendix A. Supplementary Material

Supplementary data are available free of charge at https://doi.org/10.1016/j.bioorg.XXXX.XX.XXX.Calculations of druglike properties of compounds, experimental procedures, and compound characterizationdata of 20 library members that were tested, including full ^{1}H and ^{13}C NMR spectra. Illustration of the supramolecular network and packing of **5c** in the crystal.

Notes

The authors declare no competing financial interest.

Acknowledgments

The authors would like to thank Dr. R. Rachid for her help in collecting the molecular docking data.

References

[1] World Health Organization, Definition, Diagnosis and Classification of Diabetes Mellitus and Its Complications, Switzerland: Geneva (1999).

[2] IDF Diabetes Atlas - 8th Edition. http://www.diabetesatlas.org/key-messages.html.

[3] S. Vedantham, R. Ananthakrishnan, A. M. Schmidt, R. Ramasamy, Aldose reductase, oxidative stress and diabetic cardiovascular complications,Cardiovasc. Hematol. Agents Med. Chem. 10 (2012) 234-240.

[4] M. S. Tolentino, A. J. Tolentino, M. J. Tolentino, Current and investigational drugs for the treatment of diabetic retinopathy, Expert Opin. Investig. Drugs25 (2016) 1011-1022.

[5] H. F. Jheng, M. Hirotsuka, T. Goto, M. Shibata, Y. Matsumura, T. Kawada, Dietary low-fat soy milk powder retards diabetic nephropathy progression via inhibition of renal fibrosis and renal inflammation, Mol. Nutr. Food Res.61 (2017) 1600461-1600470.

[6] American Diabetes Association, Diagnosis and classification of diabetes mellitus, Diabetes Care, 37 (2014) 81-90.

[7] R. Rubin, D.S. Strayer, E. Rubin, Rubin's Pathology: Clinicopathologic Foundations of Medicine, 6th ed. Philadelphia: Lippincott Williams & Wilkins, 4 (2012) 1081–1098.

[8] J. Michael, M.D. Fowler, Microvascular and macrovascular complications of diabetes, Clin. Diabetes 26 (2008) 77–82.

[9] K. Date, A. Satoh, K. Iida, H. Ogawa, Pancreatic α-Amylase Controls Glucose Assimilation by Duodenal Retrieval through *N*-Glycan-specific Binding, Endocytosis, and Degradation, J. Biol. Chem. 290 (2015) 17439 –17450.

[10] P.M. de Souza, P. de Oliveira Magalhães, Application of microbial α-amylase in industry-A review, Braz. J. Microbiol. 41 (2010) 850-861.

[11] https://www.intechopen.com/books/treatment-of-type-2-diabetes/pharmacological-treatments-for-type-2-diabetes.

[12] A. Chaudhury, C. Duvoor, V.S. Reddy Dendi, S. Kraleti, A. Chada, R. Ravilla, A.Marco, N.S. Shekhawat, M.T. Montales, K. Kuriakose, A. Sasapu, A. Beebe, N. Patil, C.K. Musham, G.P. Lohani, W.Mirza, Clinical Review of Antidiabetic Drugs: Implications for Type 2 Diabetes Mellitus Management, Front Endocrinol (Lausanne) 8 (2017) 1-12.

[13] J. Noble, M.O. Baerlocher, J. Silverberg, Management of type 2 diabetes mellitus. Role of thiazolidinediones, Can Fam Physician, 51 (2005) 683–687.

[14] S. Y. Rhee, H. J. Kim, S. H. Ko, K. Y. Hur, N. H. Kim, M. K. Moon, S. O. Park, B. W. Lee, K. M. Choi, J. H. Kim, Monotherapy in patients with type 2 diabetes mellitus, Diabetes Metab. J. 41 (2017) 349-356.

[15] N. Thangavel, M. Al Bratty, S. Akhtar Javed, W. Ahsan, H.A. Alhazmi, Targeting peroxisome proliferator-activated receptors using thiazolidinediones: Strategy for design of novel antidiabetic drugs, Int. J. Med. Chem. 2017 (2017) 1-20.

[16] R.L. Sawant, J.B. Wadekar, S.B. Kharat, H.S. Makasare, Targeting PPAR-γ to design and synthesize antidiabetic thiazolidines, EXCLI J. 17 (2018) 598–607.

[17] S. Chigurupati, S.A. Dhanaraj, P. Balakumar, A step ahead of PPARγ full agonists to PPARγ partial agonists: therapeutic perspectives in the management of diabetic insulin resistance, Eur. J. Pharmacol. 755 (2015) 50-57.

[18] D. Kaminskyy, A. Kryshchyshyn, D. Lesyk, Recent developments with rhodanine as a scaffold for drug discovery, Expert Opin. Drug Discov. 12 (2017) 1233-1252.

[19] S.M.Mousavi, M.Zarei, S.A.Hashemi, A.Babapoor, A.M,Amani, A conceptual review of rhodanine: current applications of antiviral drugs, anticancer and antimicrobial activities, Artif. Cells Nanomed. Biotechnol. 47 (2019) 1132-1148.

[20]K.Ramkumar, V.N.Yarovenko, A.S.Nikitina, I.V. Zavarzin, M.M.Krayushkin, L.V.Kovalenko, A. Esqueda, S.Odde, N.Neamati, Design, Synthesis and Structure-activity Studies of Rhodanine Derivatives as HIV-1 Integrase Inhibitors, Molecules 15 (2010) 3958-3992.

[21] H. Jiang, W. J. Zhang, P. H. Li, J. Wang, C. Z. Dong, K. Zhang, H. X. Chen, Z. Y.Du, Synthesis and biological evaluation of novel carbazole-rhodanine conjugates as topoisomerase II inhibitors, Bioorg. Med. Chem. Lett. 28 (2018) 1320-1323.

[22] S. P. Mandal, Mithuna, A. Garg, S. S. Sahetya, S. R. Nagendra, H. S. Sripad, M. M. Manjunath, Sitaram, M. Soni, R. N. Baig, S. V. Kumar, B. R. P. Kumar, Novel rhodanines with anticancer activity: design, synthesis and CoMSIA study, RSC Adv. 6 (2016) 58641-58653.

[23] M. Krátký, Š. Štěpánková, K. Vorčáková, J. Vinšová, Synthesis and in vitro evaluation of novel rhodanine derivatives as potential cholinesterase inhibitors, Bioorg. Chem. 68 (2016) 23-29.

[24] N. Shafii, M. Khoobi, M. Amini, A. Sakhteman, H. Nadri, A. Moradi,S . Emami, E. S. Moghadam, A. Foroumadi, A. Shafiee, Synthesis and biological evaluation of 5-benzylidenerhodanine-3-acetic acid derivatives as AChE and 15-LOX inhibitors. Enzyme Inhib. Med. Chem. 30 (2015) 389-395.

[25] N. Hotta,N. Sakamoto,Y. Shigeta,R. Kikkawa,Y. Goto,Clinical investigation of epalrestat, an aldose reductase inhibitor, on diabetic neuropathy in Japan: multicenter study,J. Diabetes Complications 10 (1996) 168-172.

[26] G. Bansala, S. Singh, V. Monga, P. V. Thanikachalama, P. Chawlaa, Synthesis and biological evaluation of thiazolidine-2,4-dione-pyrazole conjugates as antidiabetic, anti-inflammatory and antioxidant agents, Bioorg. Chem. 92 (2019) 103271-103287.

[27] L. Sun , P. Wang , L. Xu , L. Gao , J. Li , H. Piao, Discovery of 1,3-diphenyl-1H-pyrazole derivatives containing rhodanine-3- alkanoic acid groups as potential PTP1B inhibitors, Bioorg. Med. Chem. Lett. 29 (2019) 1187–1193.

[28] G. C. Wang, Y. P. Peng, Z. Z. Xie, J. Wang, M. Chen, Synthesis, α-glucosidase inhibition and molecular docking studies of novel thiazolidine-2,4-dione or rhodanine derivatives, Med. Chem. Comm. 8 (2017), 1477-1484.

[29] A. Barakat, M. S.Islam, H. M.Ghawas,A. M. Al-Majid, F. F. El-Senduny, F. A. Badria,Y. A. M. M. Elshaier, H. A. Ghabbour, Substituted spirooxindole derivatives as potent anticancer agents through inhibition of phosphodiesterase 1, RSC Adv. 8 (2018) 14335-14346.

[30] S. Haddad, S. Boudriga, F. Porzio, A. Soldera, M. Askri, D. Sriram, P. Yogeeswari, M. Knorr, Y. Rousselin,; M. Kubicki, Synthesis of novel dispiropyrrolothiazoles by three-component 1,3-dipolar cycloaddition and evaluation of their antimycobacterial activity, RSC Adv.4 (2014) 59462-59471.

[31]E. Garcia Prado, M. D. Garcia Gimenez, R. De la Puerta Vazquez, J. L. Espartero Sanchez, M. T. Saenz Rodriguez, Antiproliferative effects of mitraphylline, a pentacyclic oxindole alkaloid of Uncaria tomentosa on human glioma and neuroblastoma cell lines, Phytomedicine. 14 (2007) 280–284.

[32] S. Haddad, S. Boudriga, T. N. Akhaja, J. P. Raval, F. Porzio, A. Soldera, M. Askri, M. Knorr, Y. Rousselin, M. M. Kubicki, D. Rajani, A strategic approach to the synthesis of functionalized spirooxindole pyrrolidine derivatives: in vitro antibacterial, antifungal, antimalarial and antitubercular studies, New J. Chem., 39 (2015) 520-528.

[33] Y. Arun, K. Saranraj, C. Balachandran, P. T. Perumal, Novel Spirooxindole-Pyrrolidine Compounds: Synthesis, Anticancer and Molecular Docking Studies, Eur. J. Med. Chem. 74 (2014) 50–64.

[34] A. I. Almansour, R. S. Kumar, N. Arumugam, A. Basiri, Y. Kia, M. A. Ali,M. Farooq, V. Murugaiyah, A facile ionic liquid promoted synthesis, cholinesterase inhibitory activity and molecular modeling study of novel highly functionalized spiropyrrolidines, Molecules 20 (2015) 2296-2309.

[35] R. Murugan, S. Anbazhagan, S. S. Narayanan, Synthesis and in vivo antidiabetic activity of novel dispiropyrrolidines through [3+2] cycloaddition reactions with thiazolidinedione and rhodanine derivatives. Eur. J. Med. Chem. 44 (2009) 3272–3279.

[36] S. V.Kurbatov, V. V. Zarubaev, L. A. Karpinskaya, A. A. Shvets, M. E. Kletsky, O. N. Burov, P. G. Morozov, O. I. Kiselev, V. I. Minkin, Synthesis and antiviral activity of bis-spirocyclic derivatives of rhodanine, Russ. Chem. Bull., Int. Ed. 63 (2014) 1130-1136.

[37] Y. X. Song, D. M. Du, Asymmetric Construction of Bispiro[oxindole-pyrrolidine-rhodanine]s via Squaramide-Catalyzed Domino Michael/Mannich [3 + 2] Cycloaddition of Rhodanine Derivatives with *N*-(2,2,2-Trifluoroethyl)isatin Ketimines, J. Org. Chem. 83 (2018) 9278-9290.

[38] S. Boudriga, S. Haddad, V. Murugaiyah, M. Askri, M. Knorr, C. Strohmann, C. Golz, Three-Component Access to Functionalized Spiropyrrolidine Heterocyclic Scaffolds and Their Cholinesterase Inhibitory Activity, Molecules 25 (2020) 1963-1985.

[39] F. L. Gouveia, R. M. de Oliveira, T. B de Oliveira, I. M. da Silva, S. C. do Nascimento, K. X. de Sena, J. F. de Albuquerque, Synthesis, antimicrobial and cytotoxic activities of some 5-arylidene-4-thioxo-thiazolidine-2-ones, Eur. J. Med. Chem. 44 (2009) 2038–2043.

[40] S. Boudriga, S. Haddad, M. Askri, A. Soldera, M. Knorr, C. Strohmannd, C. Golz, Highly diastereoselective construction of novel dispiropyrrolo[2,1-a]isoquinoline derivatives via multicomponent 1,3-dipolar cycloaddition of cyclic diketones-based tetrahydroisoquinolinium N-ylides, RSC Adv. 9 (2019) 11082–11091.

[41] H. Gazzeh, S. Boudriga, M. Askri, A. Khatyr, M. Knorr, C. Strohman, C. Golz, Y. Rousselin, M. Kubicki, Stoichiometry-controlled cycloaddition of nitrilimines with unsymmetrical exocyclic

dienones: microwave-assisted synthesis of novel mono- and dispiropyrazoline derivatives,RSC Adv.6 (2016) 49868-49875.

[42] S. Haddad, S. Boudriga, F. Parzo, A. Soldera, M. Askri, M. Knorr, Y. Rousselin, M. M. Kubicki, K. Golz, C. Strohmann, Regio- and Stereoselective Synthesis of Spiropyrrolizidines and Piperazines through Azomethine Ylide Cycloaddition Reaction, J. Org. Chem. 80 (2015) 9064–9075.

[43] K.N. Houk, The Role of Secondary Orbital Interactions in Cycloaddition Reactions, Tetrahedron Lett. 30 (1970) 2621–2624.

[44] S. Boudriga, B. Elmhawech, M. Askri, Straightforward and Highly Diastereoselective Synthesis of a New Set of Functionalized Dispiropyrrolidines Involving Multicomponent 1,3-Dipolar Cycloaddition with Azomethine Ylides. J. Het. Chem. 56 (2019) 1748–1756.

[45] D.H. Ess, K.N. Houk, Distortion/Interaction Energy Control of 1,3-Dipolar Cycloaddition Reactivity, J. Am. Chem. Soc. 129 (2007) 10646–10647.

[46] K. Kaleshkumar, R. Rajaram, N. Gayathri, T. Sivasudha, G. Arun, G. Archunan, B. Gulyás, P. Padmanabhan, Muscle extract of Arothron immaculatus regulates the blood glucose level and the antioxidant system in high-fat diet and streptozotocin induced diabetic rats. Bioorg. Chem. 90 (2019) 103072.

[47] V.B. Nguyen, A.D. Nguyen, Y.-H. Kuo, S. L. Wang, Biosynthesis of α-glucosidase inhibitors by a newly isolated bacterium, Paenibacillus sp. TKU042 and Its effect on reducing plasma glucose in a mouse model. Int. J. Mol. Sci. 18 (2017) 700.

[48] C. Hansawasdi, J. Kawabata, T. Kasai, α-Amylase Inhibitors from Roselle (Hibiscus sabdariffa Linn.) Tea, Biosci. Biotechnol. Biochem. 64 (2000) 1041–1043.

[49] F. Rahim, M. Taha, H. Ullah, A. Wadood, M. Selvaraj, A. Rab, M. Sajid , S. A. A. Shah , N. Uddin, M. Gollapalli, Synthesis of new arylhydrazide bearing Schiff bases/thiazolidinone: α-Amylase, urease activities and their molecular docking studies. Bioorg Chem. 91 (2019) 103112-103122.

[50] G. Bansala, S. Singh, V. Monga, P. V. Thanikachalama, P. Chawlaa, Synthesis and biological evaluation of thiazolidine-2,4-dione-pyrazole conjugates as antidiabetic, anti-inflammatory and antioxidant agents, Bioorganic Chemistry 92 (2019)103271-103287.

[51] M. S. Altowyan, A. Barakat, A. M. Al-Majid, H.A. Al-Ghulikah, Spiroindolone Analogues as Potential Hypoglycemic with Dual Inhibitory Activity on α-Amylase and α-Glucosidase, Molecules, 24 (2019) 2342-2362.

[52] O. V. Dolomanov, L. J. Bourhis, R. J. Gildea, J. A. K. Howard, H. Puschmann, OLEX2: a complete structure solution, refinement and analysis program, J. Appl. Crystallogr. 42 (2009) 339-341.

[53] G. M. Sheldrick, SHELXT - Integrated space-group and crystal-structure determination, Acta Crystallogr. A, 71 (2015) 3-8.

[54] G. M. Sheldrick, Crystal structure refinement with SHELXL. Acta Cryst. *C*71 (2015), 3–8.

[55] E.O. Yeye, K.M. Khan, S. Chigurupati, A. Wadood, A.U. Rehman, S. Perveen, M.K. Maharajan, S. Shamim,S. Hameed, S.A. Aboaba, M.Taha, Syntheses, in vitro α-amylase and α-glucosidase dual inhibitory activities of 4-amino-1, 2, 4-triazole derivatives their molecular docking and kinetic studies, Bioorg. Med. Chem. 28 (2020) 115467-115475.

[55] Hamden, K.; Keskes, H.; Belhaj, S.; Mnafgui, K.; Feki, A.; Allouche, N. Inhibitory potential of omega-3 fatty and fenugreek essential oil on key enzymes of carbohydrate-digestion and hypertension in diabetes rats, Lipids Health Dis. 10 (2011) 226-236.

[56] Stalin A., Kandhasamy S., Kannan B.S., Verma R.S., Ignacimuthu S., Kim Y., Shao Q., Chen Y., Palani P. (2020) Synthesis of a 1,2,3-bistriazole derivative of embelin and evaluation of its effect on high-fat diet fed-streptozotocin-induced type 2 diabetes in rats and molecular docking studies. Bioorganic Chemistry 96:103579. DOI: https://doi.org/10.1016/j.bioorg.2020.103579.

[57] Xiao J.-Q., Liu W.-Y., Sun H.-p., Li W., Koike K., Kikuchi T., Yamada T., Li D., Feng F., Zhang J. (2019) Bioactivity-based analysis and chemical characterization of hypoglycemic and antioxidant components from Artemisia argyi. Bioorganic Chemistry 92:103268. DOI: https://doi.org/10.1016/j.bioorg.2019.103268.

[58] M. Sobeh, M.F. Mahmoud, M.A.O. Abdelfattah, H. A. El-Beshbishy, A. M. El-Shazly, M. Wink, Albizia harveyi: phytochemical profiling, antioxidant, antidiabetic and hepatoprotective activities of the bark extract, Med. Chem. Res. 26 (2017) 3091-3105.

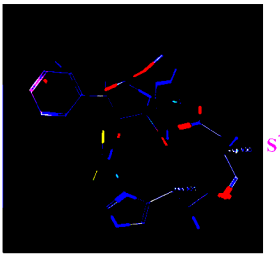

Molecular docking

SAR points

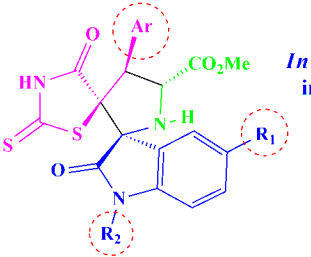

{19 examples}

Novel rhodanine-fused spiro[pyrrolidine-2,3'-oxindole]

In vitro α-amylase inhibition study

In vivo experiments

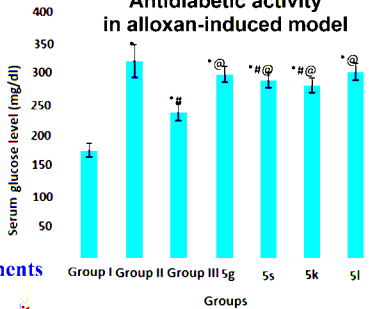

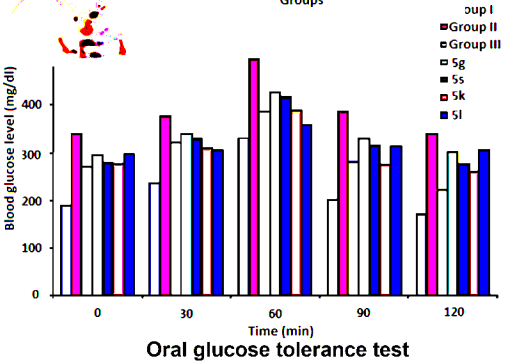

- One pot reaction
- High yield and selectivity
- Wide substrate scope
- Bioactive compounds